

**NASA CONTRACTOR  
REPORT**

NASA CR-1246



NASA CR-1246  
C.1

006055J



LOAN COPY: RETURN TO  
AFWL (WLIL-2)  
KIRTLAND AFB, N MEX

# EXPERIMENTS ON A HIGH POWER, PULSED, CONSTRICTED ARC HEATER

*by Rolf Dethlefsen*

*Prepared by*  
GENERAL DYNAMICS CORPORATION  
San Diego, Calif.  
*for Ames Research Center*

NASA CR-1246  
TECH LIBRARY KAFB, NM



0060551

EXPERIMENTS ON A HIGH POWER, PULSED,  
CONSTRICTED ARC HEATER

By Rolf Dethlefsen

Distribution of this report is provided in the interest of  
information exchange. Responsibility for the contents  
resides in the author or organization that prepared it.

Issued by Originator as Report No. GDC-DBE68-008

Prepared under Contract No. NAS 2-4665 by  
GENERAL DYNAMICS CORPORATION  
San Diego, Calif.

for

NATIONAL AERONAUTICS AND SPACE ADMINISTRATION

---

For sale by the Clearinghouse for Federal Scientific and Technical Information  
Springfield, Virginia 22151 - CFSTI price \$3.00



## FOREWORD

The reported work was performed under Contract NAS 2-4665 for the Magnetoplasmdynamics Branch of the NASA Ames Research Center. This work was performed in support of the hypersonic wind tunnel development program under the technical cognizance of Mr. C. E. Shepard. The work was started in December 1967. The report manuscript was finished in July 1968.

The author wishes to acknowledge many technical suggestions of Mr. C. E. Shepard which proved to be very helpful to this work. Mr. Shepard made the comparison of data from the pulsed and the continuous facility. He supplied Figures 20, 21, 22. Special acknowledgment is given to Mr. J. P. Tinkham for contributing to the design and for building the test facility. His enthusiasm was a major factor in the progress of the work.



## EXPERIMENTS ON A HIGH POWER, PULSED, CONSTRICTED ARC HEATER

By Rolf Dethlefsen  
Convair Div. of General Dynamics

### SUMMARY

Pulsed experiments on a high power constricted arc with axial flow have been performed by discharging a lumped parameter transmission line composed of a number of capacitors and inductors. The advantages of a pulsed experiment are experimental convenience because no water cooling is needed, and much lower cost due to savings in power supply investment. It was found that for a 26 cm dia. and 135 cm long arc constrictor a 5 msec pulse time is sufficient in order to achieve steady flow conditions during the latter half of the pulse.

The arc current ranged from 1.8 to 3.6 KA with a flow rate of nitrogen from 5 to 40 g/sec. The constrictor inlet pressure and arc voltage were measured. Time integrated measurements were made of the radiative heat flux leaving the quartz constrictor. Also, the heat was measured which is absorbed in the quartz constrictor walls. The constricted arc heater exhausted into a low pressure volume. Some photos were taken of the supersonic exhaust interacting with a wedge and a blunt body.

Several important phenomena were discovered during the course of the study. High speed photographs revealed flow instabilities. Under certain circumstances, the arc did not fill the tube; instead a relatively concentrated arc filament fluctuated about the tube. A swirling gas inlet was found to be effective in reducing arc instabilities. Evidence for strong Maecker cathode jets was also found. Impinging on the constrictor walls, these jets could lead to increased erosion, or shorting of segments in a continuous facility. It was found that the cathode jets could be eliminated by using a cathode with simultaneous arc attachment on four parallel tungsten rods. This four-pin cathode also showed lower cathode erosion than a cathode with a single tungsten rod. In addition, a cascading circuit for gas breakdown triggering of the long tube was developed which is superior to wire explosion triggering.

The data taken on the pulsed facility agree with those taken on a similar facility which operates in a continuous mode in the NASA Ames Research Laboratory. The pulsed facility is able to operate in a wider range of parameters. It is feasible and advantageous to use a pulsed version of the high power constricted arc heater for pursuing those research topics where data can be collected within a few msec.



## TABLE OF CONTENTS

	<u>Page</u>
I. INTRODUCTION	1
II. APPARATUS	2
1. Pulsed Power Supply and Gas Flow Supply	2
2. Synchronization and Triggering	5
3. Arc Constrictor	7
III. EXPERIMENTAL RESULTS	10
1. Measurements	10
2. Data	13
3. Comparison of the Pulsed Arc Voltage and Pressure Data with that of a Continuous Facility	26
4. Photographic Investigations	32
IV. CONCLUDING SECTION	43
V. REFERENCES	46



# LIST OF ILLUSTRATIONS

<u>Figure</u>		<u>Page</u>
1.	Schematic of the pulsed, high power, constricted arc experiment.	4
2.	Calibration check of pressure in plenum chamber and instant of time when arc fires. Applied pressure is 290 psi.	5
3.	Pulsed constricted arc with gas breakdown triggering.	6
4.	Cathode assembly with sonic orifices and pressure transducers.	8
5.	Copper segment in arc constrictor wall.	9
6.	Anode design for pulsed constricted arc.	11
7.	Calibration of sonic orifices. Mass flow rate of nitrogen $\dot{m}$ as function of stagnation pressure $P_s$ in plenum chamber.	12
8.	Oscillograms of current, arc voltage, and upstream pressure. Gas breakdown triggering with flow rate of 13.2 g/sec nitrogen and 2.15 KA current.	14
9.	Oscillograms of current, arc voltage, and upstream pressure. 3 mil aluminum wire triggered with flow rate of 42.6 g/sec nitrogen and 2.1 KA current.	15
10.	Oscillograms of upstream pressure. Gas flow of nitrogen with strong vortex and gas breakdown triggering.	17
11.	Inlet pressure of constricted arc heater $P_1$ as function of nitrogen flow rate $\dot{m}$ with/without vortex gas flow.	18
12.	Inlet pressure $P_1$ of constricted arc heater as function of nitrogen flow rate $\dot{m}$ .	19
13.	Arc voltage $U$ as function of nitrogen flow rate $\dot{m}$ .	20
14.	Arc voltage $U$ as function of nitrogen flow rate $\dot{m}$ .	21
15.	Inlet pressure $P_1$ of constricted arc heater as function of nitrogen flow rate.	22
16.	Arc voltage $U$ as function of nitrogen flow rate $\dot{m}$ .	23
17.	Arc voltage $U$ as function of nitrogen flow rate $\dot{m}$ .	24

# LIST OF ILLUSTRATIONS CONT'D.

<u>Figure</u>	<u>Page</u>
18. Calorimeter geometry for measuring wall heat flux.	25
19. Heat flux absorbed in quartz constrictor wall $q_a$ and heat flux transmitted through quartz wall $q_r$ as function of nitrogen flow rate $\dot{m}$ .	27
20. Voltage between cathode and 54" station $U_3$ as function of nitrogen flow rate $\dot{m}$ .	29
21. Inlet pressure $P_1$ as function of nitrogen flow rate $\dot{m}$ .	30
22. Total heat flux to constrictor wall $q_t$ as function of nitrogen flow rate $\dot{m}$ .	31
23. Different cathodes tested with the pulsed arc.	32
24. Arc attachment on the three cathodes of Fig. 23. 17.5 g/sec nitrogen flow, 3.2 KA.	33
25. Arc attachment on the cathode of Fig. 23C. 17.4 g/sec nitrogen flow, 3.0 KA, $t = 0$ at start of the current pulse.	35
26. Arc attachment on the cathode of Fig. 23B with pointed end face. 16 g/sec nitrogen flow, 2 KA, lower photo is retouched in order to show the cathode jet more clearly.	36
27. High speed film displaying the time history of the pulsed arc with axial flow. 11 g/sec nitrogen flow, 2 KA. Position about 20 cm downstream of cathode.	37
28. High speed film displaying the time history of the pulsed arc with axial flow. 39 g/sec nitrogen flow, 1.9 KA. Position at the cathode end of the constrictor.	39
29. High speed film displaying the time history of the pulsed arc with axial flow containing a strong vortex. 46 g/sec nitrogen flow, 1.9 KA. Position at the cathode end of the constrictor.	40
30. A wedge exposed to the exhaust stream of the pulsed arc heater. Position of leading edge about 4 cm from exit plane of anode. 30.7 g/sec nitrogen flow, 3.5 KA current, exposure time about 1 $\mu$ sec.	41
31. A 0.5"-diam. rod exposed crosswise to the exhaust stream of the pulsed arc constrictor. Position about 2 cm from exit plane of the anode. Frame separation about 80 $\mu$ sec, exposure time about 1 $\mu$ sec.	42

## I. INTRODUCTION

The reentry test facilities as developed by NASA call for higher and higher power levels in the constricted arc heater section. The next generation of arc heaters is to be designed for a 30 MW power level. Also the test-section impact pressure must be increased. Such a device that is capable of steady-state operation constitutes a large investment in power supplies and water-cooled arc constrictor sections. Although the theory of the arc constrictors is well developed and good agreement has been achieved between the theory and experiments<sup>1,2</sup> in the range below 5 MW of power and below 7 atm of pressure, at higher values of power and pressure uncertainties exist in the theory which arise from the effects of radiative heat transfer, plasma turbulence, and arc column instabilities. For this reason, it is of interest to conduct further research on the constricted arc at high power levels.

The objective of the work covered by this report is to investigate the feasibility of performing the needed research with a pulsed high power arc facility. Experiments on a pulsed arc constrictor are meaningful if a quasi-stationary flow of gas through the constricted arc can be obtained in a time which is shorter than the discharge time of the pulsed power supply.

A lumped parameter transmission line consisting of discharge capacitors and inductances is capable of providing very high levels of electric power for the constricted arc over short periods of time. The cost of these pulsed power supplies is very modest compared to continuously operating facilities. A pulsed arc heater does not need water cooling. The same applies for instrumentation immersed into the arc plasma. Therefore, it is possible to obtain data relatively conveniently and quickly from a pulsed experiment.

Three additional considerations add interest to this approach:

1. The continuous heat flux that can be tolerated by water-cooled electrodes is limited by the rate of heat transfer at the solid-liquid interface. This limit is set at about 10 KW/cm<sup>2</sup> for water. The theoretical limit set by the thermal conduction and melting temperature of a 1-mm-thick copper electrode is 35 KW/cm<sup>2</sup>. In a pulsed system these limits are removed, so that experiments could be performed in a regime where no present day continuous device can operate. This could be a step leading to the development of liquid-metal-cooled electrodes.

2. A capacitor discharge line can also be pulsed into a continuously operating arc heater. This would raise the exit enthalpy for a few msec above presently achievable values without exceeding the tolerable heat flux to the walls. This could be of value to actual reentry tests.

3. The walls of a pulsed arc constrictor can be made from quartz. This allows photographic investigations which are difficult to perform on a continuous device.

The feasibility of the pulsed approach can be judged from two criteria.

1. Attaining a quasi-stationary flow through the arc constrictor is indicated by a constant pressure level at the inlet to the constrictor.

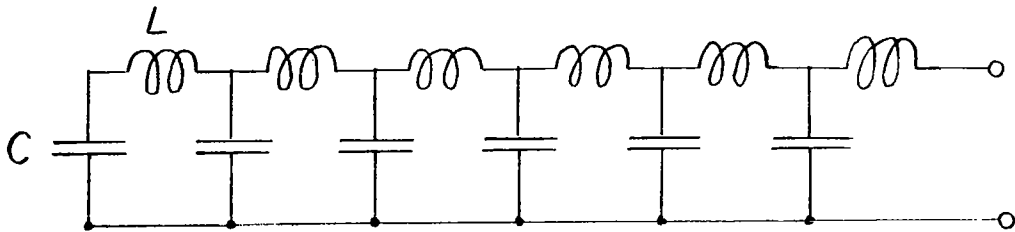
2. For comparison, data are taken on the pulsed device in a range of parameters accessible to the continuous facility at the NASA Ames Research Center.

## II. APPARATUS

### 1. Pulsed Power and Gas Flow Supply

The use of a pulsed arc current reduces the cost of the power supplies considerably. But, care has to be taken that the events are properly synchronized, and also that steady-state conditions are reached for those parameters which are to be investigated.

A nearly rectangular arc current pulse is obtained from the discharge of a lumped parameter transmission line. Such a line consists of  $N$  capacitors  $C$  and inductors  $L$  connected as follows:



If the number of sections is sufficiently large the governing relations are identical to the well-known discharge characteristics of a length of transmission cable.<sup>3</sup>

The impedance of the pulse line is given by  $Z_0 = \sqrt{\frac{L}{C}}$ .

If the pulse line is discharged into a matched load a rectangular current pulse with a duration of  $T = 2N\sqrt{CL}$  and a magnitude of  $I = \frac{V_0}{2Z_0}$  is

generated. Here  $U$  is the charging voltage. The discharge current can be varied:

- (1) By choosing different levels of charging voltage.
- (2) By having variable inductors.

Varying the inductance also changes the impedance and the pulse duration.

The schematic of the pulsed, high power, constricted arc experiment is shown in Fig. 1. The pulsed power supply consists of sixty  $15\ \mu\text{F}$  capacitors and inductors with about  $108\ \mu\text{H}$ . The inductors are 60 turn coils of gauge 6 wire with a length of 18 cm, inner diameter of 6 cm and outer diameter of 11 cm. These coils were cast in epoxy because the mechanical forces exerted on the windings can be appreciable at high currents. We found that the ohmic resistance of the inductor coils caused a drooping of the current during the pulse time. In order to achieve a constant pulse current the inductance of the pulse coils was changed. To the first coil in the line 20 turns of gauge 6 wire were added. To the succeeding coils in the line a linearly decreasing number of turns was added. The inductance of the coils near the end of the line was decreased by inserting pieces of iron pipe into the inner diameter. (This is effective because the skin-effect excludes magnetic flux from the area occupied by the iron pipe). This method of tailoring the pulse coil inductance proved to be effective in changing the arc current pulse. A capacitor was added to the front of the discharge line in order to obtain a fast rising current pulse with an initial overshoot in magnitude. This is beneficial for triggering the arc.

The impedance of the pulse line is about  $2.7\ \Omega$ . The arc resistance generally has a lower value. This unbalance of impedances can lead to current reversal. For improving the impedance match a  $0.7\ \Omega$  "Glow Bar" carbon resistor was added to the circuit. Switching of the arc current was achieved with a mercury ignitron type 7703. The trigger voltage is obtained from the discharge line voltage by use of a voltage divider. The ignitron fires when switch  $S_1$  is closed. Switch  $S_1$  is a vacuum switch with a 40 KV stand-off voltage. For safety reasons the discharge line is enclosed in a steel mesh cubicle. The pulse current is carried to the arc constrictor via high voltage coaxial cable. The current magnitude is 3.6 KA at 20 KV charging voltage with a pulse duration of 5 msec.

The flow of nitrogen is pulsed on for about 0.2 sec. The electrical actuation of the shut-off valve (type MV 36, made by Marotta Valve Corp., Boonton, N. J.) was changed in order to suit our needs. The reservoir consists of high pressure gas cylinders with about 8 cu ft volume. It is important to keep gas lines between the reservoir and the valve short and without constriction. The valve is directly attached to the small plenum chamber which feeds four sonic orifices. The pressure rise in this plenum chamber is shown in the following oscillogram. We see that after 70 msec a constant pressure is attained. At this point in time the arc can be fired.

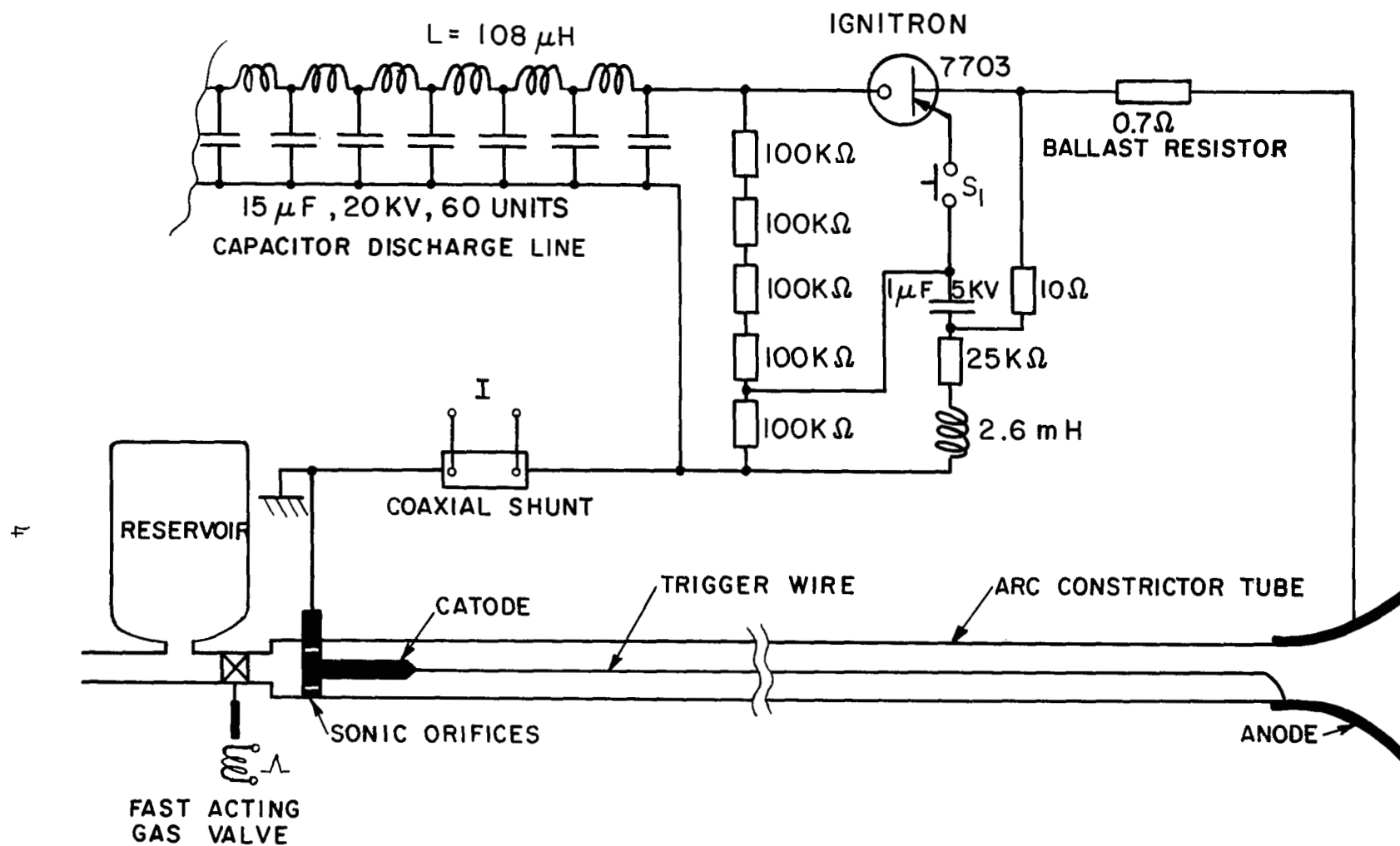


Fig. 1. Schematic of the pulsed, high power, constricted arc experiment.

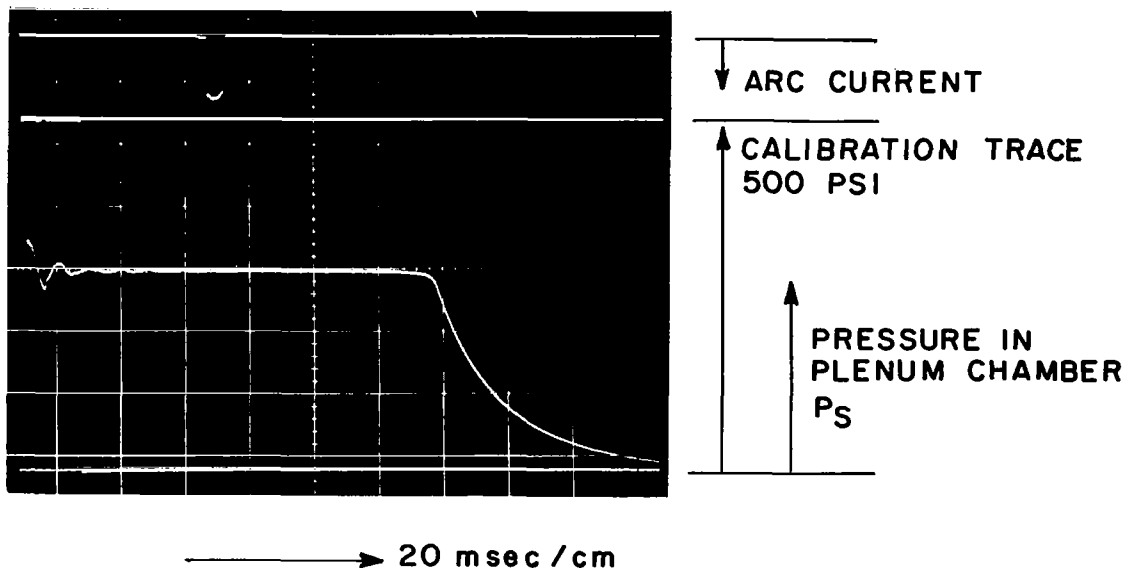


Fig. 2. Calibration check of pressure in plenum chamber and instant of time when arc fires. Applied pressure is 290 psi.

## 2. Synchronization and Triggering

The gas valve is activated from a hand switch which is well insulated for safety reasons. A simple circuit with relays delays the signal to fire the ignitron by a time which is variable in a range of about 100 msec.

Triggering initially was achieved with a 2 mil diameter aluminum wire strung between anode and cathode. When the ignitron fires, this wire explodes. The generated metal plasma starts the arc. By the time when steady flow conditions have been attained the metal plasma has been swept out of the tube. Triggering with a wire is inconvenient, and splashes of molten metal tend to deteriorate the constrictor walls. Therefore gas breakdown triggering was tried. The arrangement shown in Fig. 3 was very successful except for the case of high flow rate. Before firing, the arc constrictor is pumped down to a pressure near 1 mm of mercury. When a steady flow of cold nitrogen gas is flowing through the constrictor the pressure at the cathode reaches values in the range of 0.2 atm. Gas in the full length of the tube will not break down with charging voltages

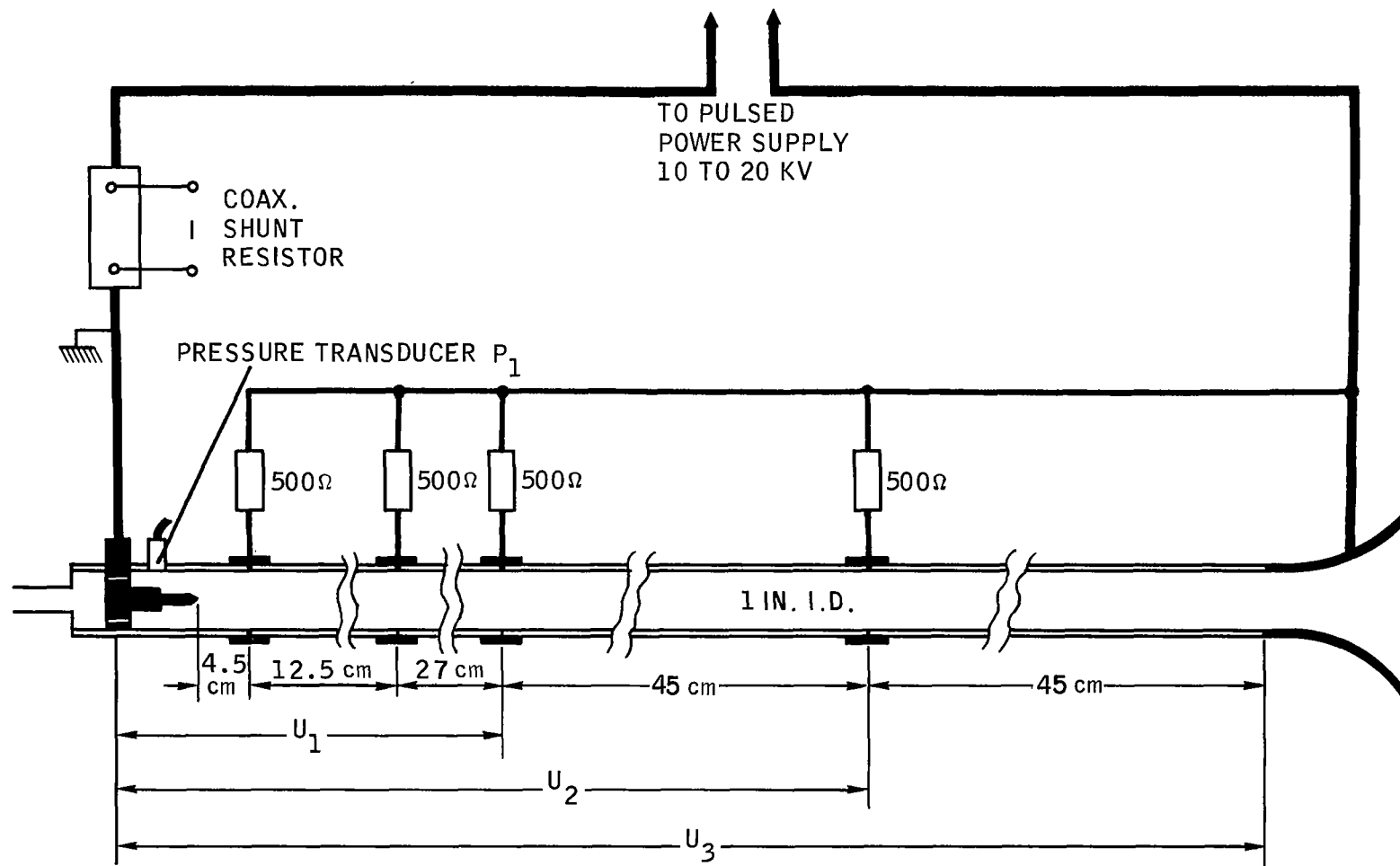


Fig. 3. Pulsed constricted arc with gas breakdown triggering.



between 10 and 20 KV. Copper segments are inserted into the constrictor wall at various distances from the cathode. Each of these segments is connected to the anode by a 500  $\Omega$  resistor. When the ignitron fires, the first segment is able to break down the gas inside the constrictor. The resulting arc current is limited to values near 30 amp. by the 500  $\Omega$  resistor. The ionized arc plasma, being swept downstream, breaks down the following segments in succession until breakdown occurs to the anode, at which time the full arc current starts to flow. At high flow rates it takes up to 1 msec until the high power arc is established. This mode of triggering worked very well except for the case of high gas flow rates and low charging voltage and is adaptable to varied conditions.

### 3. Arc Constrictor

The arc constrictor nominally is 56" long and has 1" inner diameter with a thickness of the quartz tube wall of about 2.4 mm. The dimensions varied somewhat for different shipments of quartz. Where more precise dimensions are critical they are given with the data. It was found that quartz walls are superior to either pyrex or vycor glass.

The design details of the inlet section of the arc constrictor are shown in Fig. 4.

A 0.5" pipe connects the plenum chamber to the fast-acting gas valve. The gas is metered from the plenum chamber into the arc constrictor through 4 sonic orifices. See the view cut AA. These orifices issue gas jets in a tangential direction. These orifices can either be aligned such that all of them blow in the same direction, thus creating a strong vortex, or they can be aligned as is shown in Fig. 4. Then they create a turbulent gas flow without swirl.

Figure 4 shows the cathode assembly and the first segment of the triggering scheme shown in Fig. 3. The sealing gaskets are made either from silicon rubber or from teflon. It was found that the radiative heat flux deteriorates the silicon rubber. Silicon rubber therefore was used only in places where it could be shielded from the arc radiation. Teflon did not deteriorate noticeably. The cathode consists of 1/8" diameter, 2% thoriated tungsten rods pressed into a copper holder. The erosion rate of the tungsten is low, and the rods are readily replaced if needed. (See Fig. 23) Piezoelectric pressure transducers are installed with an isolating insert. A passage of 1/8" diameter and 1/4" long transmits the pressure to the transducer and prevents destruction of the transducer by the arc. This procedure is recommended by the manufacturer and is claimed not to impair the time response in the present range of interest.

Figure 5 shows the design of those segments in the constrictor wall which were used to measure the electric potential drop along the axis of the constricted arc.

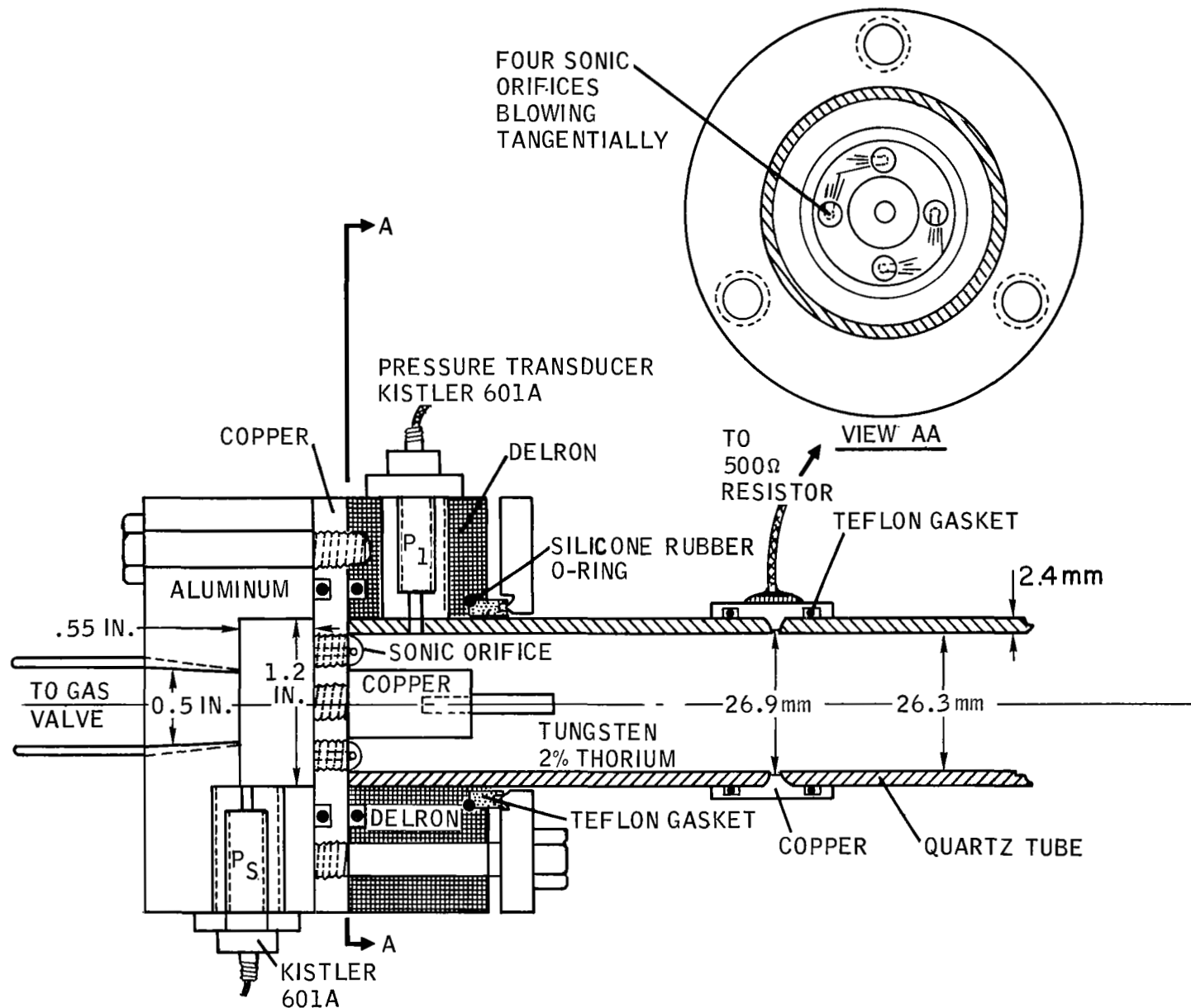


Fig. 4. Cathode assembly with sonic orifices and pressure transducers.

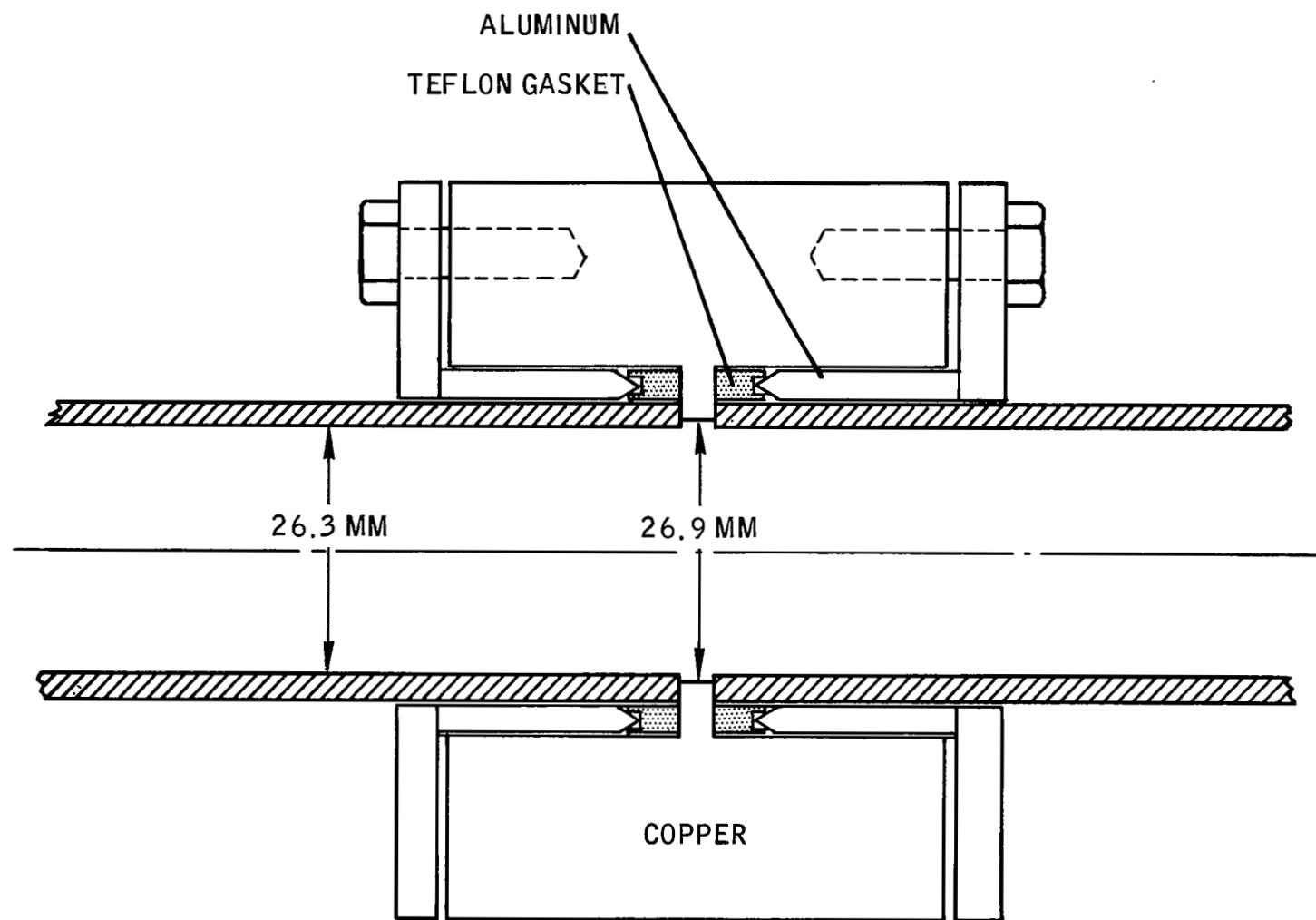


Fig. 5. Copper segment in arc constrictor wall.

Figure 6 shows the design of the anode. The cylindrical anode is machined from solid copper. Initially the arc-heated gases issuing from the anode were exhausted into the atmosphere. It proved to be desirable to exhaust into an evacuated volume because the smaller amount of gas contained in the constrictor at the instant of starting the arc discharge results in a reduced pressure overshoot. All reported data were taken with the constrictor exhausting into a 10'-long glass tube with 6' I.D. A mechanical forepump, electrically isolated, was used to pump this glass tube down to a pressure of about 1 mm Hg.

### III. EXPERIMENTAL RESULTS

#### 1. Measurements

The values of arc current, pressure, and arc voltage were taken from the traces of Tektronix oscilloscopes, Model 564 and 503. The arc current was measured with a shunt resistor. This resistor was constructed from coaxial copper conductors. The voltage sensing leads were attached to the inside of the hollow center conductor. This guarantees that the voltage readout circuit is inductively decoupled from the current-carrying circuit in order to obtain the true waveform of the pulsed arc current. This high current shunt was calibrated with instruments of 0.5% accuracy.

The pressure readings were obtained from piezoelectric transducers, type Kistler 601A, with charge amplifier Model 503. The charge amplifiers were mounted in a box containing a desiccant, since they are adversely affected by humidity. The calibration of the pressure transducers with their charge amplifiers was checked by comparing the output with direct pressure measurements taken from a mechanical gauge with an accuracy of better than 1% in the range used. An example of the calibration is shown in Fig. 2. The arc voltage was recorded with Tektronic voltage dividers Model P6015. The accuracy of the current, pressure, and arc voltage measurements is principally limited by the accuracy of the scope traces.

The gas flow was metered to the constrictor through four sonic orifices with a pressure ratio that always was maintained at a value greater than two. Under this condition the mass flow rate of nitrogen is a function of the stagnation pressure in the plenum chamber only. (The orifice size and the stagnation temperature are constant.) The diameter of the four orifices is about 0.1 cm. The mass flow rate versus stagnation pressure calibration is shown in Fig. 7. A Heise pressure gauge with 0.1% accuracy at full scale (1000 psi) and a Rotameter with 0.5% accuracy at full scale (19 g/sec) were<sup>4</sup> used for this calibration. The linear relationship is expected from theory. Therefore it is safe to extrapolate this calibration to higher values of mass flow rate.

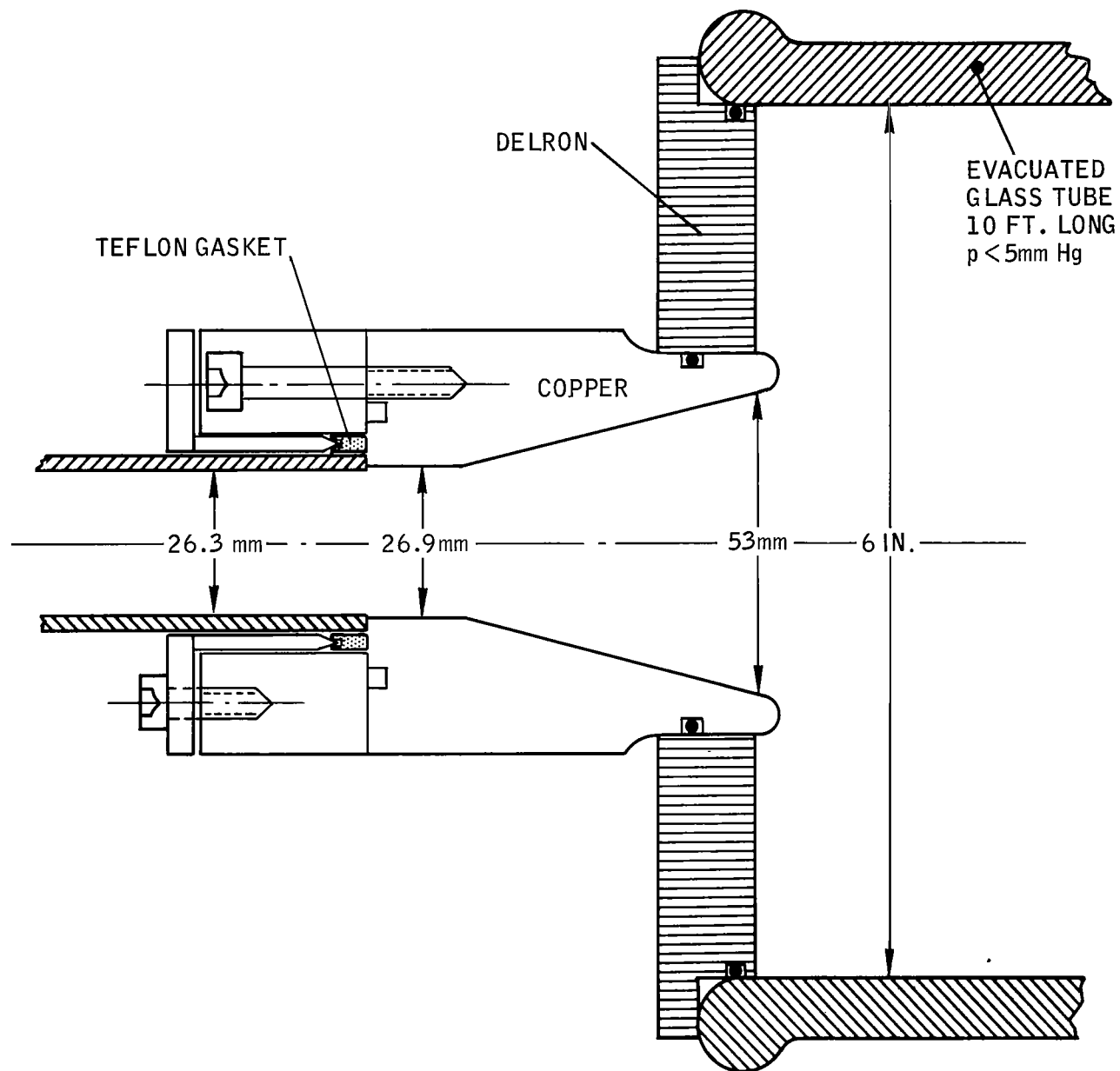


Fig. 6. Anode design for pulsed constricted arc.

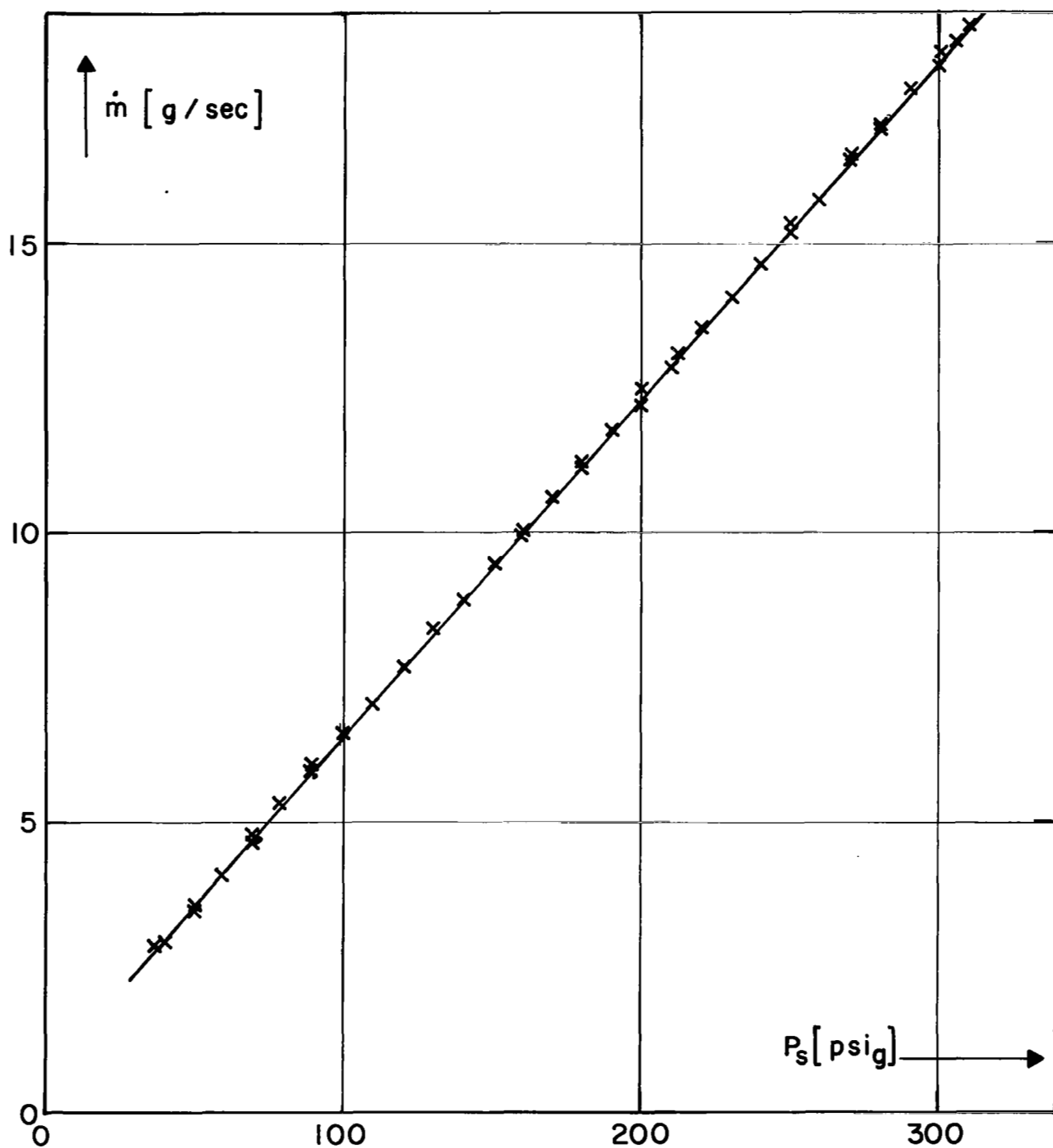


Fig. 7. Calibration of sonic orifices. Mass flow rate of nitrogen  $\dot{m}$  as function of stagnation pressure  $P_s$  in plenum chamber.

The heat flux measurements were obtained from the measured temperature rise of bodies with known thermal mass. The temperature rise was measured with iron-constantan thermocouples. The standard calibration tables were used.<sup>5</sup> The calibration was checked by exposing the thermocouples to known temperatures between 20°C and 100°C. The cold junctions were placed in a bath of melting ice. The readout was given by a potentiometer-type printing recorder with an accuracy of about 2% in the range used. These heat flux measurements represent values which are averaged over the pulse time of 5 msec.

Photographic investigations were carried out with a Dynafax camera which allowed a maximum rate of 26,000 frames per sec with an exposure time of about 1  $\mu$ sec and a frame separation of about 38  $\mu$ sec.

## 2. Data

The primary objective of this study is to determine the feasibility of obtaining quasi-stationary conditions in the pulsed arc experiment. Typical oscillograms of the pulsed current, arc voltage and upstream pressure are given in the following paragraph. This may enable the reader to use his own judgement for estimating the time required to reach steady flow conditions.

Subsequently the values of pressure and arc voltage, measured near the end of the pulse, are presented. These will be compared with those taken on the constricted arc heater operating at the NASA Ames Research Laboratory.

(A) Oscillograms of pulsed arc current, voltage and constrictor inlet pressure.- Figure 8 shows the trace of current, upstream pressure, and arc voltage in three axial positions. The arc current pulse shows an approximately rectangular shape. Also the arc voltage and pressure show well-defined plateau values, indicating quasi-stationary conditions. The starting phase is characterized by an overshoot of pressure and of the arc voltage. Following this, the nearly constant plateau values of pressure and voltage fall off sharply when the arc current extinguishes. The peaks in the voltage trace at the end of the pulse are related to the cut off of the ignitron. Figure 8 indicates that under favorable conditions a quasi-stationary test time of 3 msec can be obtained out of a pulse length of about 5 msec. Favorable conditions exist if gas breakdown triggering can be employed and if a low gas flow rate is chosen.

Figure 9 shows oscillograms taken with a high gas flow rate and with a trigger wire used for starting the arc. The trigger wire explosion generates a steep overshoot in pressure. The quasi-stationary test time is shortened to about 1 msec. At high mass flow the traces show increased random fluctuations. These are probably correlated to the arc column instability that was found to be pronounced at high mass flow rates. The high frequency hash on the pressure traces appears to be a resonance of the

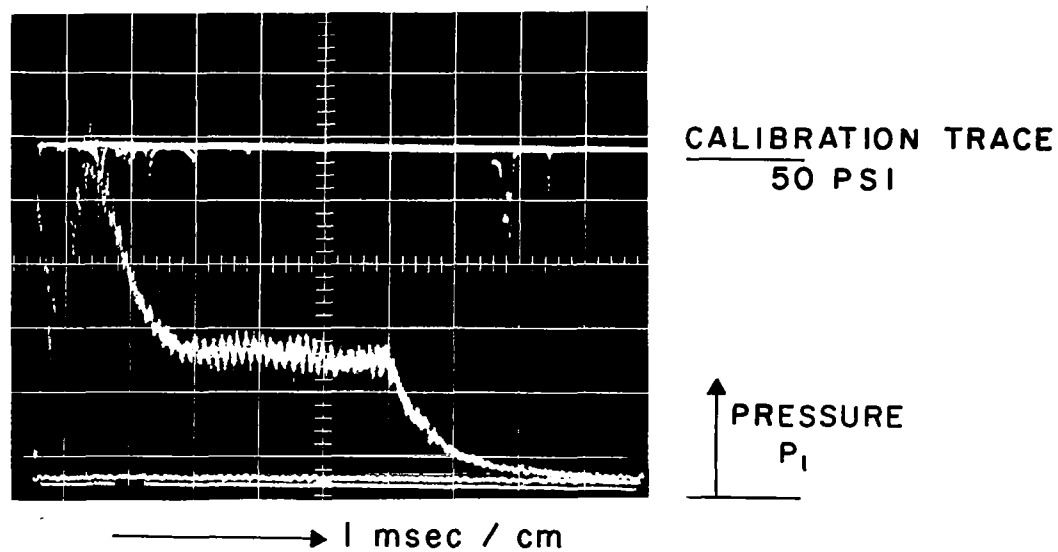
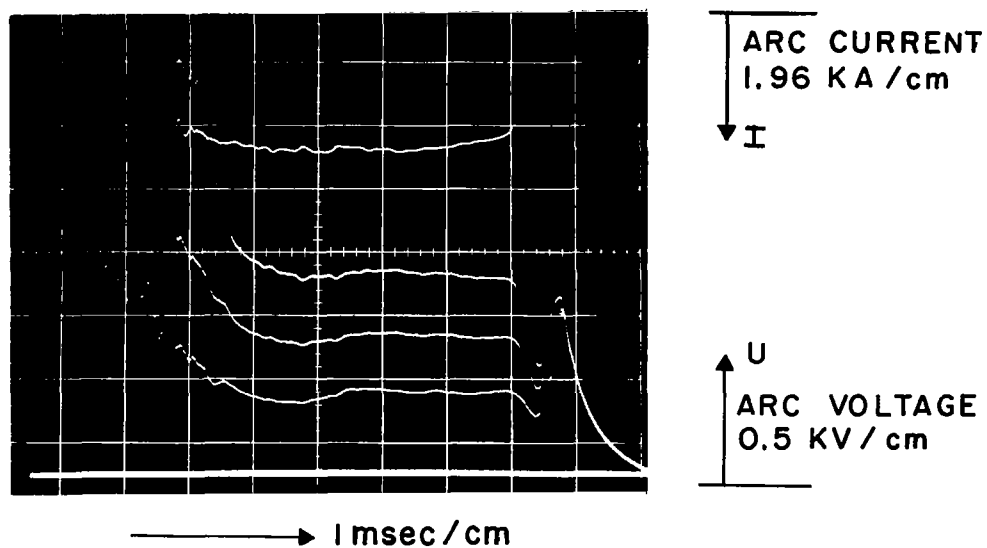


Fig. 8. Oscillograms of current, arc voltage, and upstream pressure. Gas breakdown triggering with flow rate of 13.2 g/sec nitrogen and 2.15 KA current.



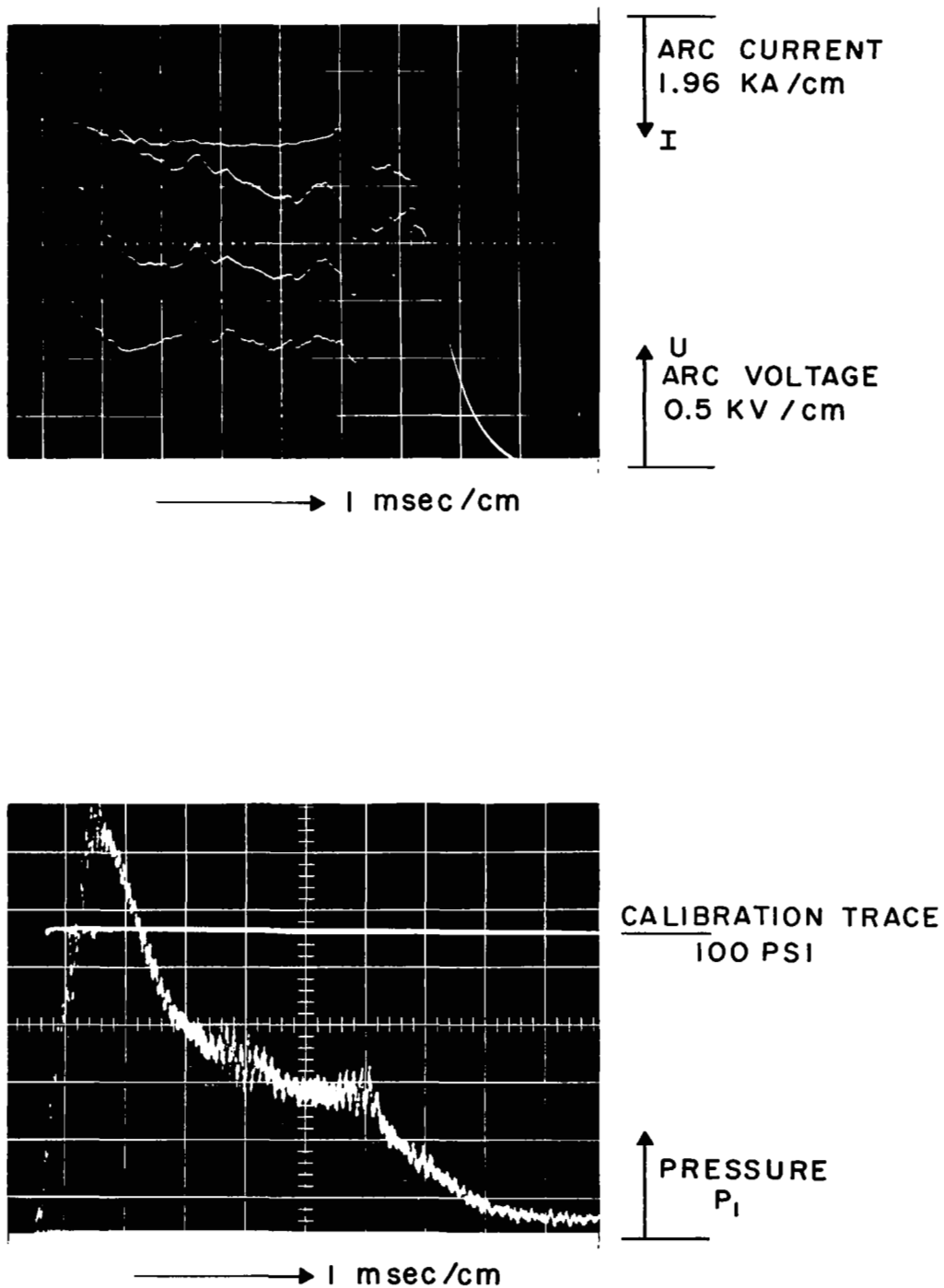


Fig. 9. Oscillograms of current, arc voltage, and upstream pressure. 3 mil aluminum wire triggered with flow rate of 42.6 g/sec nitrogen and 2.1 KA current.

duct connecting the pressure transducer to the arc constrictor. In isolated cases ablation of the walls or of the O-ring seals proved to be a problem. This was evidenced from pressure signals which went through a minimum and showed a rising value toward the end of the pulse.

Figure 10 shows two pressure signals that were obtained with a gas flow containing a strong vortex. In this case the four gas inlet nozzles were turned such that they exhausted tangentially in like sense. The noise on the pressure signals is decreased, but a plateau of constant pressure is not obtained. Instead, the pressure trace maintains a slight negative slope. Although the reason is not known, it may be due to an interaction of the vortex with the transient gas dynamic phenomena.

The lower oscillogram of Fig. 10 shows that the gas breakdown triggering allows a sizeable reduction of the initial pressure overshoot. The low current trigger arcs which are drawn by the various copper segments allow a more gradual rise of the pressure.

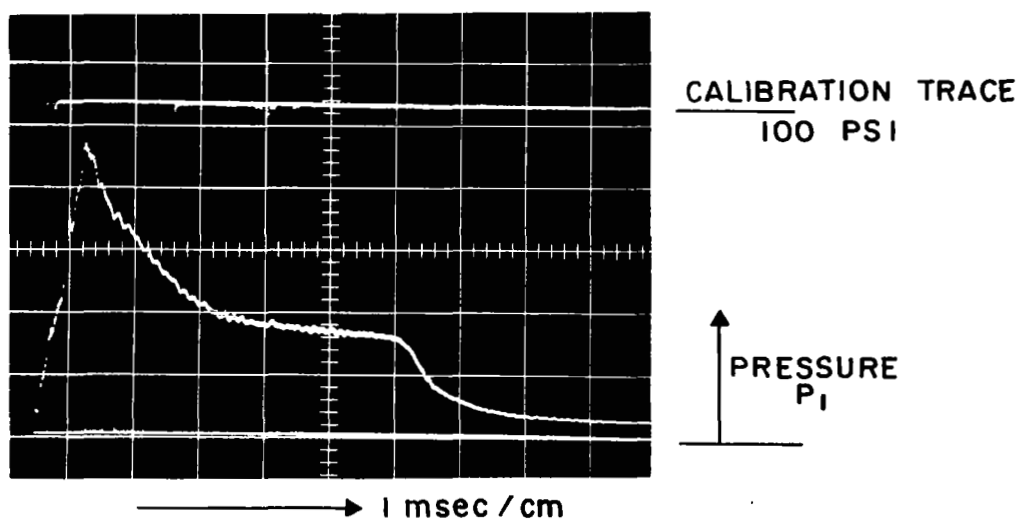
(B) Values of arc voltage and constrictor inlet pressure measured near the end of the current pulse.- A series of tests was performed in order to gain data for a comparison with the continuous arc heater facility of similar dimensions, operating at the NASA Ames laboratory. The following graphs show the values of pressure and voltage as determined from the quasi-stationary phase of the pulsed arc gas flow interaction.

Figure 11 shows the effect of the vortex in the gas flow on the measured upstream pressure. The presence of the vortex raises the measured pressure. This is also true for the case of a cold gas flow without an arc. It is concluded that the increased pressure is due to a radial pressure gradient generated by the vortex. The vortex had no pronounced effect on the measured arc voltage.

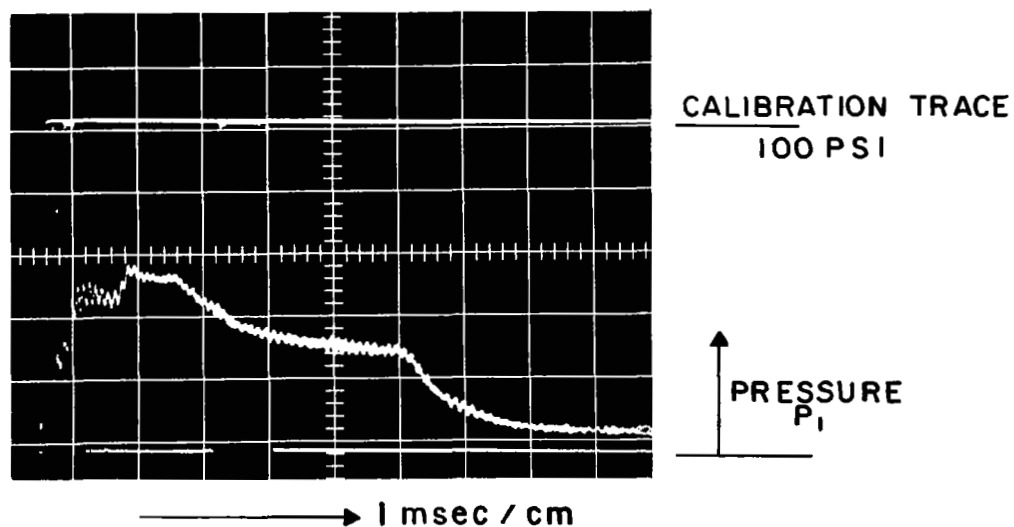
All subsequent data were taken with a gas flow containing no vortex.

A set of data taken earlier in the test program is shown in Figs. 12, 13, 14. The upstream pressure shows a nearly linear increase with mass flow rate. With increasing current the pressure increases less than linear. Also the arc voltage shows a nearly linear increase with mass flow rate. (For a definition of  $U_1$ ,  $U_2$ ,  $U_3$  see Fig. 3.) The voltage gradient is strongest near the cathode. The quartz tubes used for this test series had an inner diameter of 26.3 mm.

The results of a subsequent test series with quartz tubes of 26.4 mm I.D. are shown in Figs. 15, 16, 17. These data show the same trends as those of the earlier test series. Yet, the measured values are somewhat smaller, particularly at high flow rates. For the later test series all critical O-rings were made from teflon, thus reducing contamination. Also the calibration of mass flow rate, pressure, current and voltage was re-checked. Both sets of test data are presented in order to allow the reader



FLOWRATE 15.25 g /sec , CURRENT 3 KA



FLOWRATE 18.2 g /sec , CURRENT 2.1 KA

Fig. 10. Oscillograms of upstream pressure. Gas flow of nitrogen with strong vortex and gas breakdown triggering.

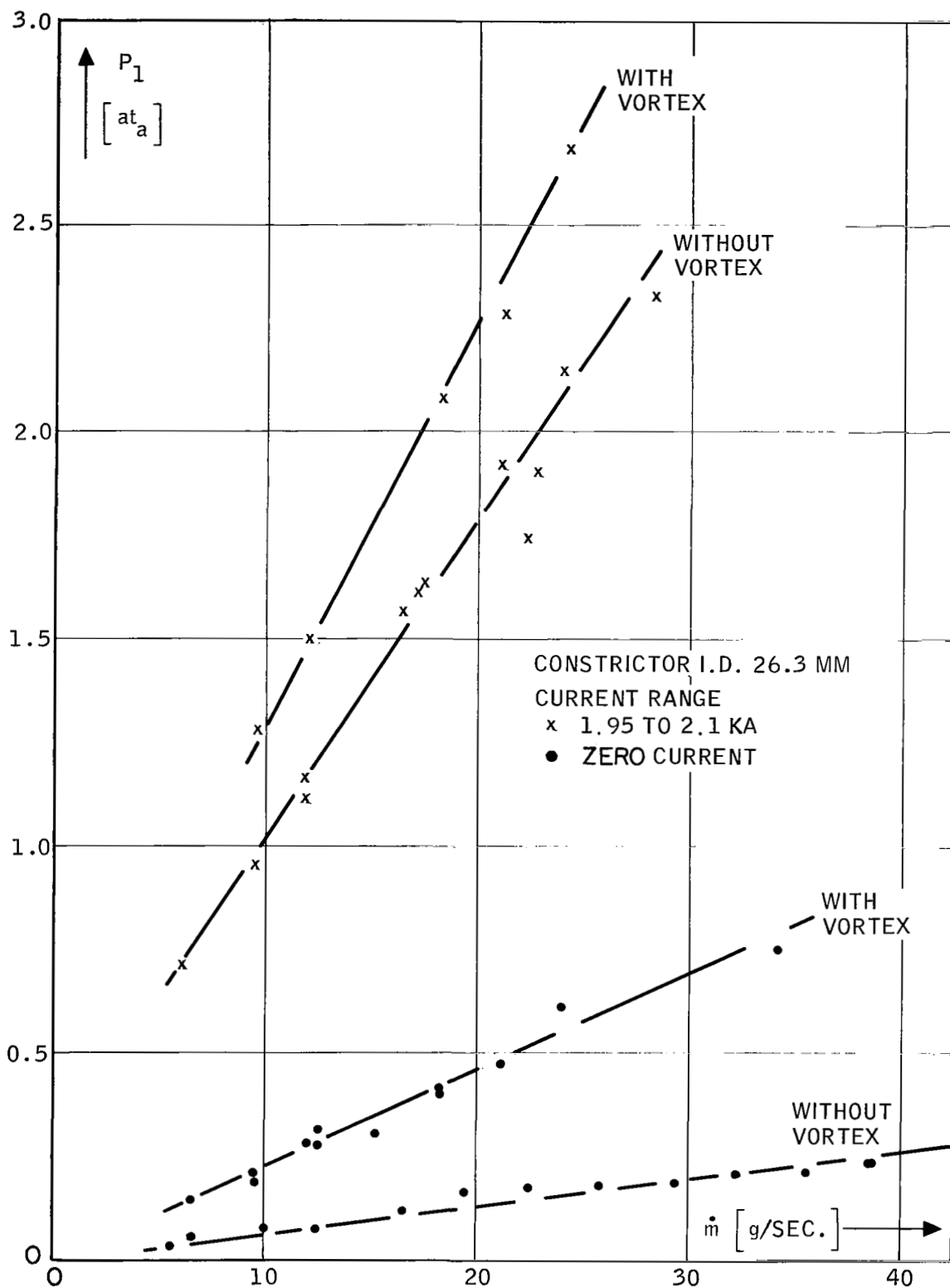
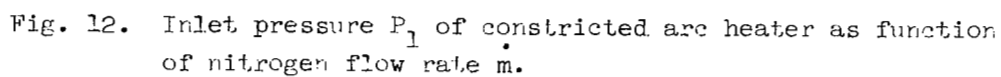


Fig. 11. Inlet pressure of constricted arc heater  $P_1$  as function of nitrogen flow rate  $\dot{m}$  with/without vortex gas flow.



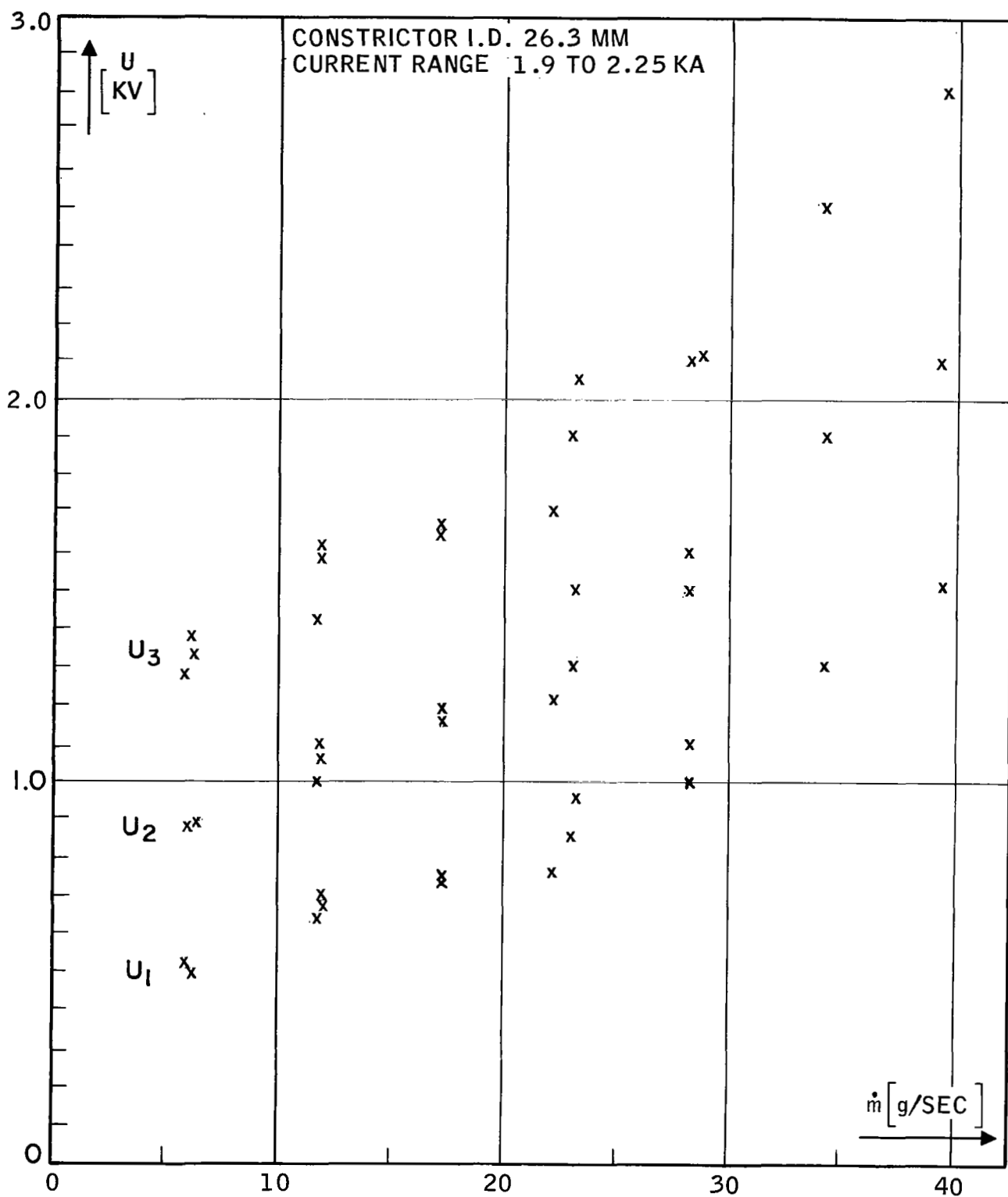


Fig. 13. Arc voltage  $U$  as function of nitrogen flow rate  $\dot{m}$ .

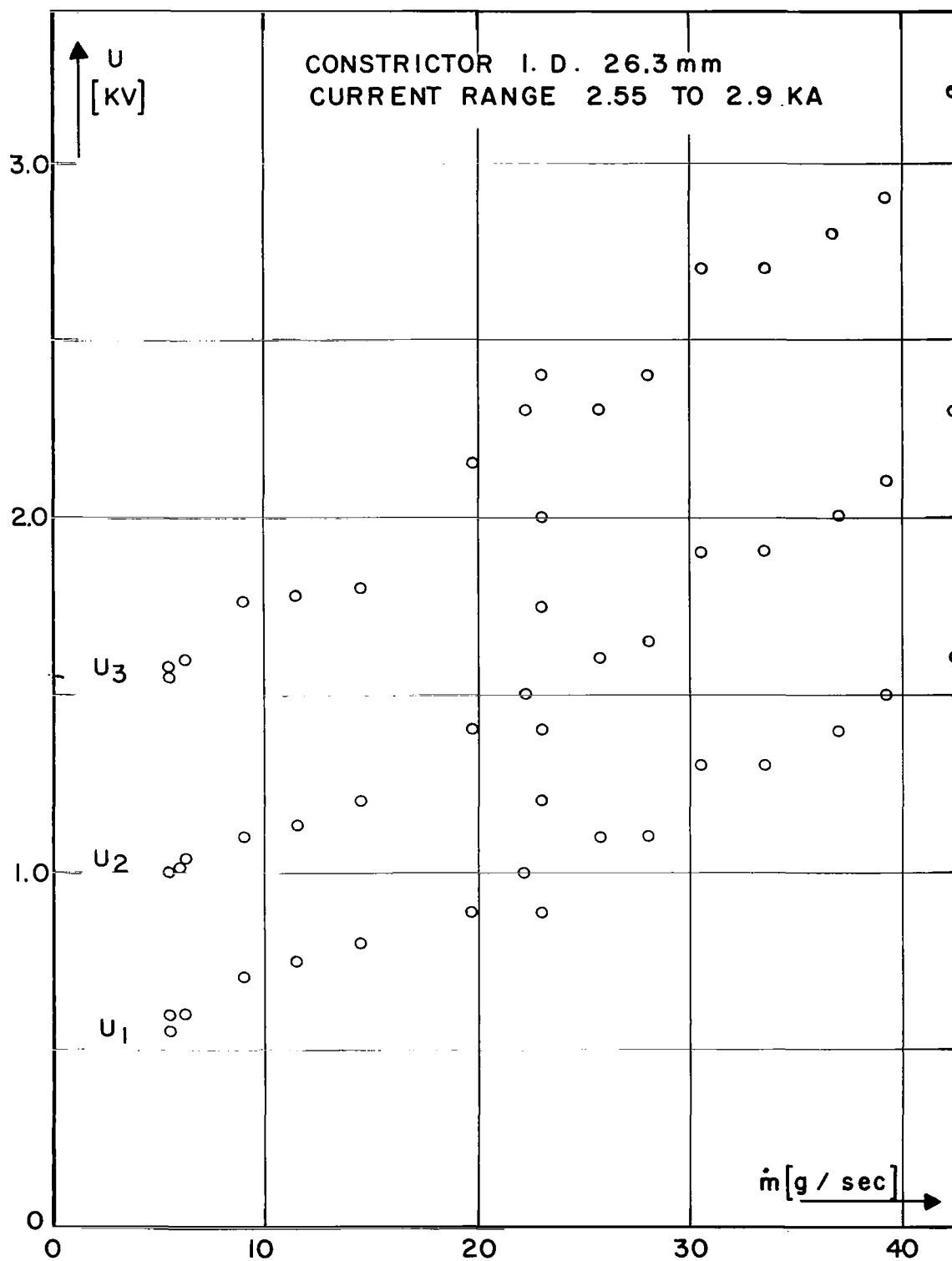


Fig. 14. Arc voltage  $U$  as function of nitrogen flow rate  $\dot{m}$ .

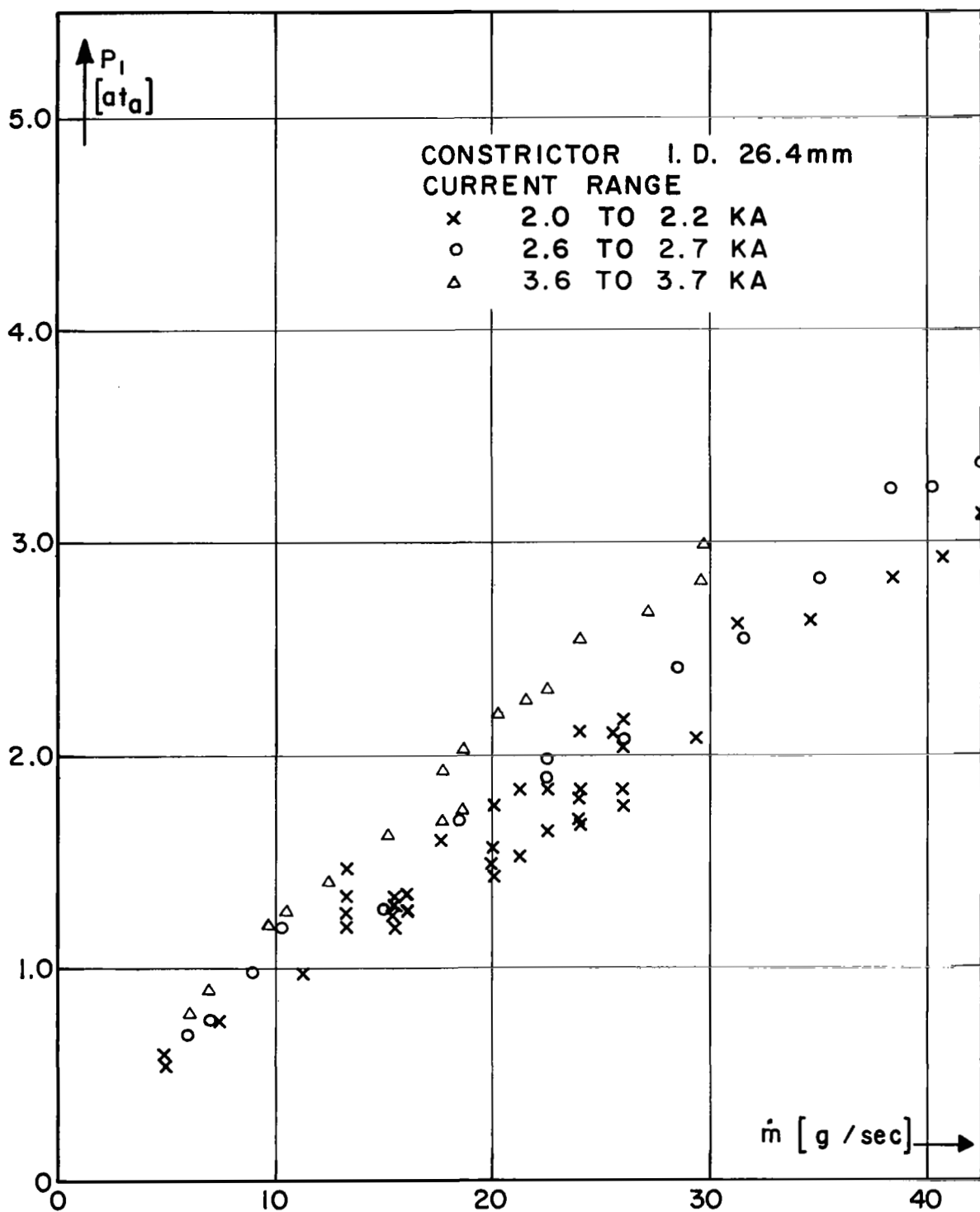


Fig. 15. Inlet pressure  $P_1$  of constricted arc heater as function of nitrogen flow rate.



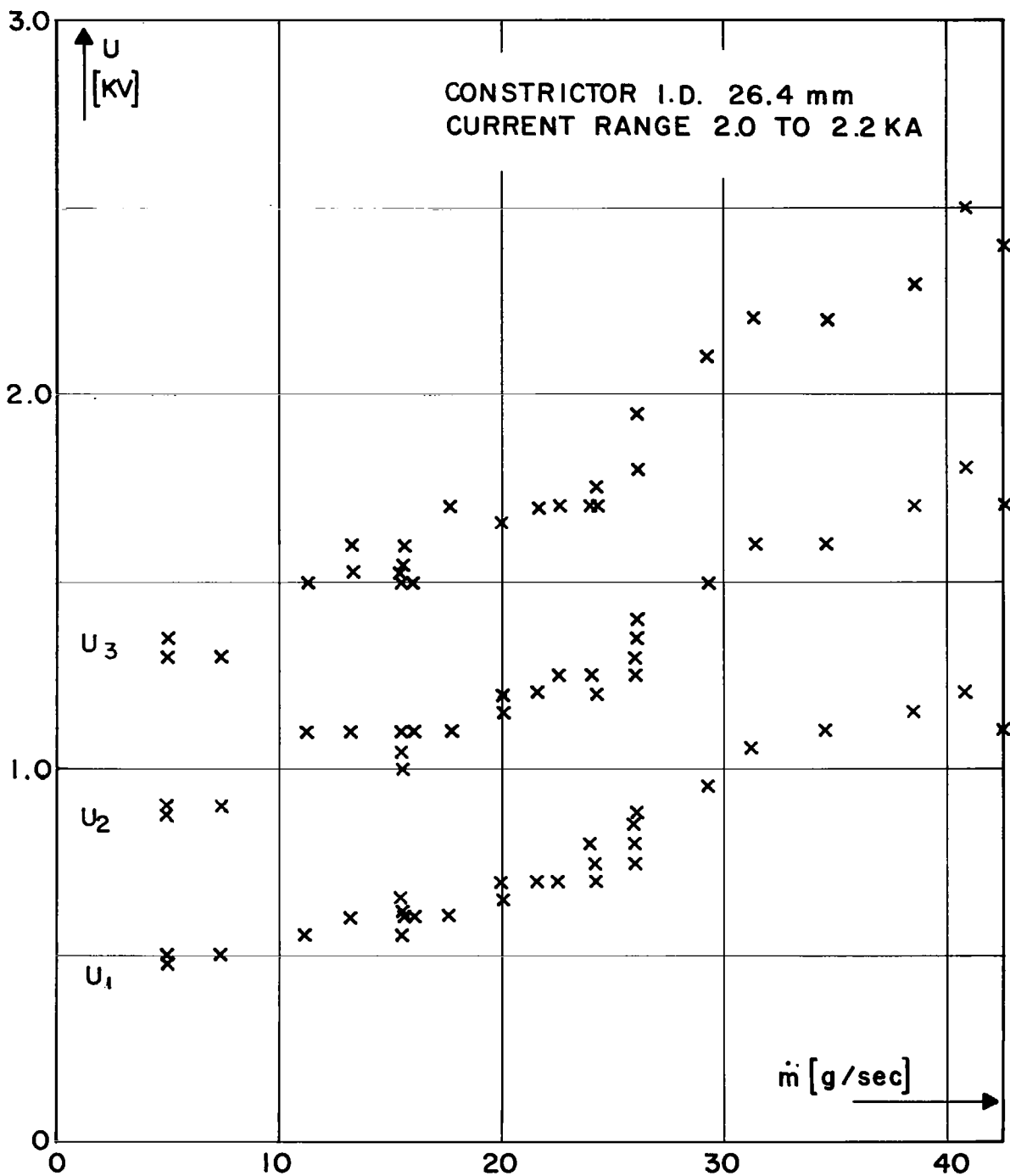


Fig. 16. Arc voltage U as function of nitrogen flow rate  $\dot{m}$ .

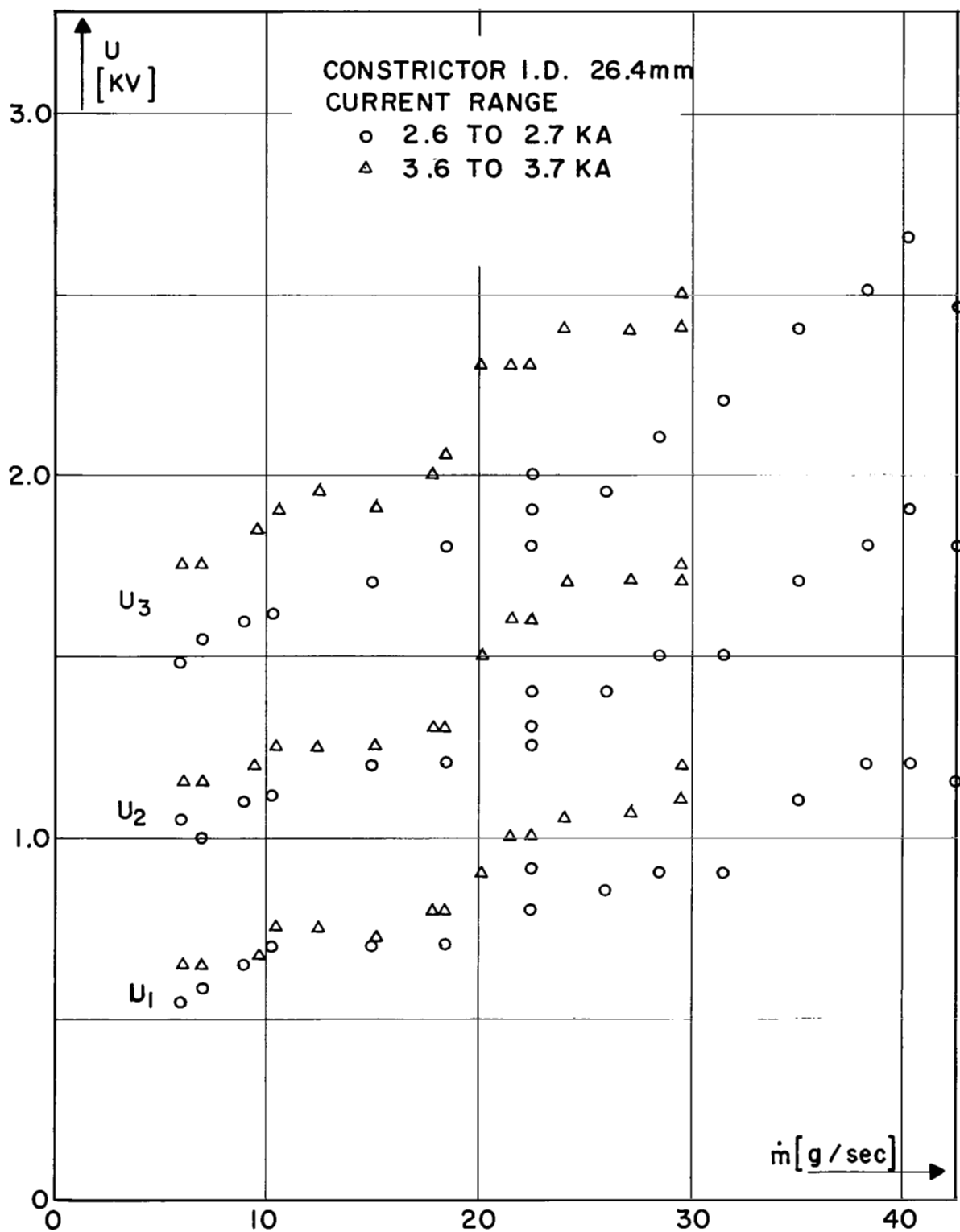


Fig. 17. Arc voltage  $U$  as function of nitrogen flow rate  $\dot{m}$ .

to make his own estimate of the range of uncertainty. The discrepancy between the data amounts to about 12%, a part of which can be explained by the larger inner diameter of the constrictor tube for the second set of data. Also, the contamination level was likely to be lower in the second set of data. (Figs. 15, 16, 17.) In the first set of data a 2% thoriated, 1/8"-diam. tungsten cathode was used. By weighing the cathode it was established that cathode erosion could have provided a maximum contamination of 5% by weight or, equivalently, about 1% per volume. The second set of data was taken with a cathode consisting of four parallel rods of 1/8" diam. tungsten, 2% thoriated. The mass loss of the cathode indicated a maximum tungsten contamination level of 1% by weight. Slight erosion of the quartz tube walls can occur at high values of gas flow rate. This is particularly pronounced near the cathode. The clear quartz becomes opaque in places where ablation occurs. Data were disregarded wherever the pressure trace indicated heavy erosion by a positive slope near the end of the pulse.

(C) Time integrated measurement of wall heat flux.- The heat flux which is absorbed in the quartz constrictor wall and the radiative heat flux which is transmitted through the quartz wall have been measured with a simple calorimeter, shown in Fig. 18. The measured temperature rise, per arc discharge, of the quartz wall and of the graphite sleeve yield values of heat flux which are time averaged over the total pulse length. Since the transient high pressure phase of the pulsed arc heater is

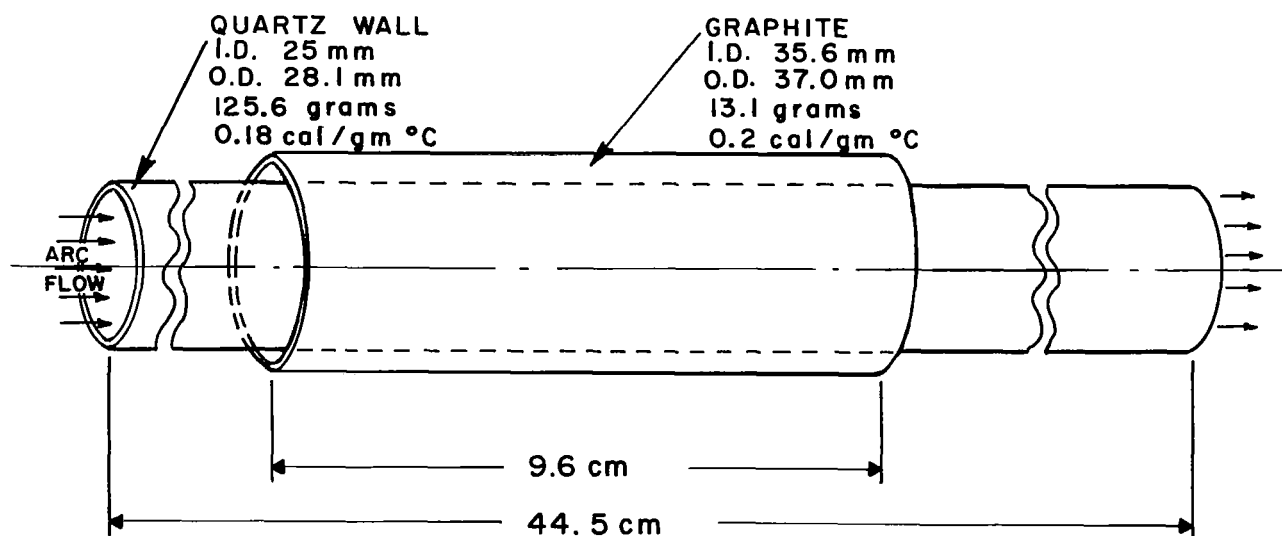


Fig. 18. Calorimeter geometry for measuring wall heat flux.

associated with a raised heat flux, it is likely that the data shown in Fig. 19 are somewhat higher than those of the stationary phase. The data indicate that about 30% of the total heat flux is transmitted through a quartz wall with 1.4 mm thickness. The radiative heat flux increases with increasing mass flow rate, due to the increased pressure in the arc discharge. The total heat flux strongly increases with raised current. The cold gas which flows through the constrictor for about 100 msec after the current pulse does not introduce any large error into the measurement of the wall absorbed heat flux. When the pulsed arc was fired near the end of the gas pulse, thus shortening the succeeding cold gas flow, no effect on the measured value of  $q_a$  was apparent. Gas breakdown triggering was used for these heat transfer measurements, thus eliminating contamination by the trigger wire metal. Erosion of the quartz tube wall could not be detected either visually or by weighing. The emitted heat flux contained a strong ultraviolet component. This was evidenced by a strong smell of ozone in the room after every discharge, particularly for runs with high mass flow rate. The emitted radiation intensity was sufficient to melt tin foils which were placed in the vicinity of the quartz constrictor.

In a side-line experiment the quartz constrictor tube was enclosed in shiny aluminum foil. The objective was to see whether this would influence the inlet pressure and the arc voltage. The radiative heat flux constitutes a sizeable fraction in the energy balance. If a part of this radiation could be returned to the arc by reflection it might be possible to observe an effect on other parameters of the arc which are governed by the energy balance. No such effect could be observed.

A secondary flow of argon is used in many similar arc heater facilities to protect the cathode from erosion. In one test series, therefore, up to 30 mol% of argon was added to the nitrogen flow in order to determine its effect on the measured parameters. There was no effect on the upstream pressure. The arc voltage and the heat absorbed in the quartz wall decreased by only about 10%. The radiative heat flux seemed to increase slightly with increasing argon content.

### 3. Comparison of the Pulsed Arc Voltage and Pressure Data with that of a Continuous Facility

The shape and size of the pulsed arc (Fig. 3) was chosen so that a direct comparison of performance could be made with the NASA, Ames Arc-Heated Planetary Gas Wind Tunnel.<sup>2</sup> Duplication of voltage, inlet-pressure of the constrictor tube, and wall heat transfer rate would provide strong evidence that the pulsed arc jet has truly reached steady-state conditions and that test results for one device could be applied to the other. Such a comparison is necessary because the oscillograms of voltage and pressure such as shown in Fig. 8 might show further change over a time period that is long compared with the oscillograph sweep. For example, there might be a long time-constant change in reaching the final flow profiles within the constrictor tube.

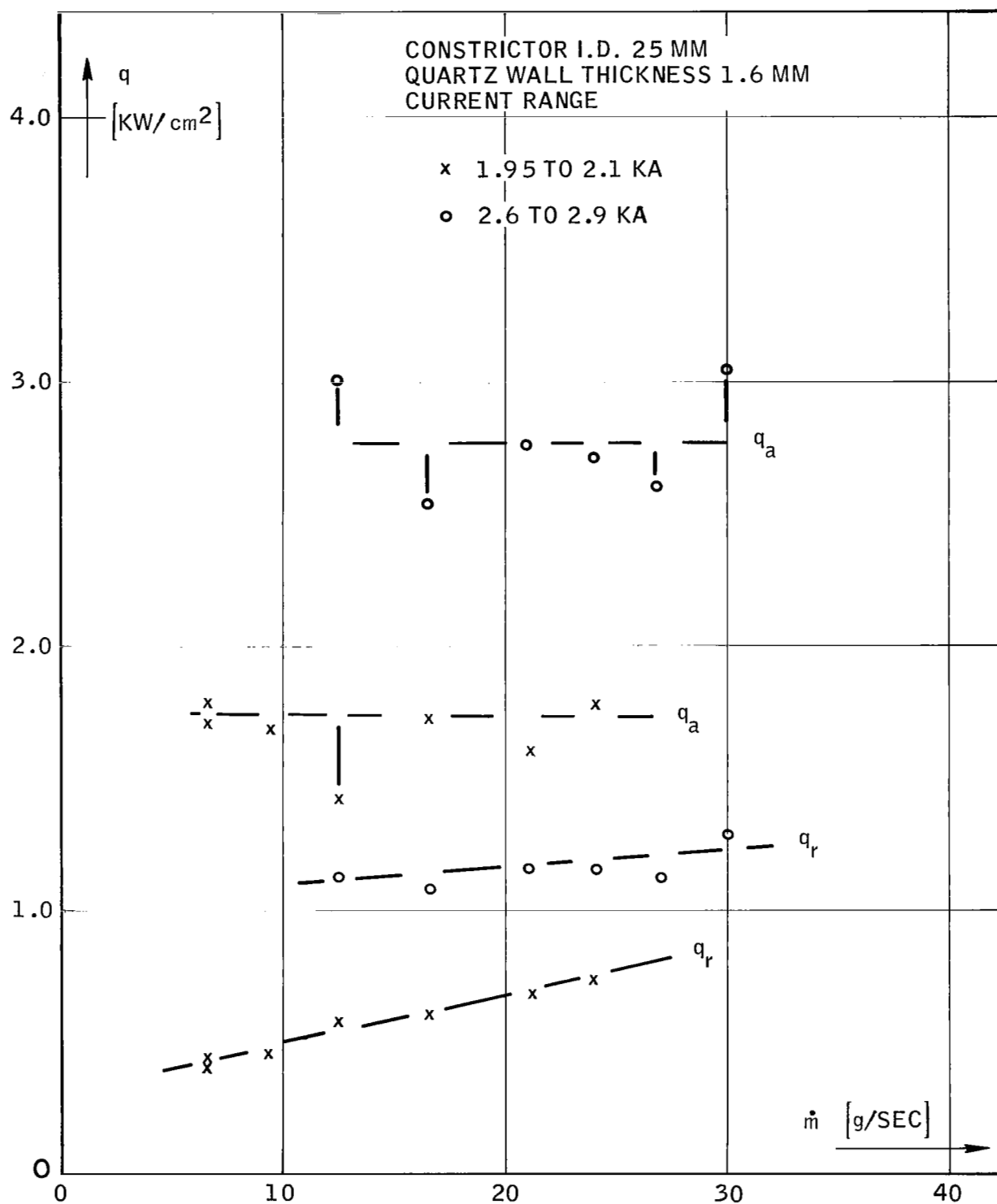


Fig. 19. Heat flux absorbed in quartz constrictor wall  $q_a$  and heat flux transmitted through quartz wall  $q_r$  as function of nitrogen flow rate  $\dot{m}$ .

Figure 20 compares the constrictor voltage,  $U_3$ , for the two arc jets. The agreement is excellent, although the scatter of the pulsed arc data is somewhat greater than desired. The larger range of flow rates for the pulsed arc jet shown in Fig. 20 also implies that a much wider range of operation is possible with this device.

The comparison of constrictor upstream pressure is complicated by differences in the constrictor size and in the method of flow injection. The effect of tube diameter,  $D$  and cross section area,  $A$  can be calculated by assuming a critical flow relationship:

$$\dot{m}/A = \text{constant} \times p H^{-0.4}$$

and by assuming that the enthalpy,  $H$  varies as  $I/D$ . Then for a given current,  $I$  and flow rate one obtains

$$p'/p = (D'/D)^{-2.4} \quad (\text{Ref. 1,2})$$

The diameter of the arc constrictor is 26.3 mm in the pulsed device and 25.4 mm in the continuous facility. This leads to a factor of 1.087 for the pressure correction. In the Ames steady-state arc jet, the nitrogen was injected with an unknown amount of swirl and was distributed over about 8 inches of constrictor length. The effect of the distributed flow injection is believed to be small, but Fig. 11 shows a large effect of the swirl on the measured pressure in the pulsed arc. In order to compare the constrictor pressure, the data of Fig. 11 for flow injection with and without swirl is compared with the steady-state arc jet pressure for a current of about 1.8 KA and a range of nitrogen flow rates. Curves faired through the pulsed arc data for strong swirl and zero swirl are seen to span the curve of the moderate swirl steady-state pressure. Fig. 21 shows a reasonably good agreement between the pressure data, taken on the pulsed and on the continuous facility, if the effect of swirl is taken into account.

The heat transfer rates of Fig. 19 are, of course, time averages over the pulse length of 5 msec.<sup>2</sup> Because the wall heat flux is known to be a strong function of pressure<sup>2</sup> and because the pressure is observed to overshoot for an appreciable part of the pulse, the integrated heat transfer rates should be higher than steady-state values.

Figure 22 shows a comparison of heat transfer rates measured on the pulsed and on the continuous arc constrictor. The measurements were taken near the midpoint of the constrictor tube. As expected, the pulsed arc data are higher than those from the continuous NASA Ames facility.

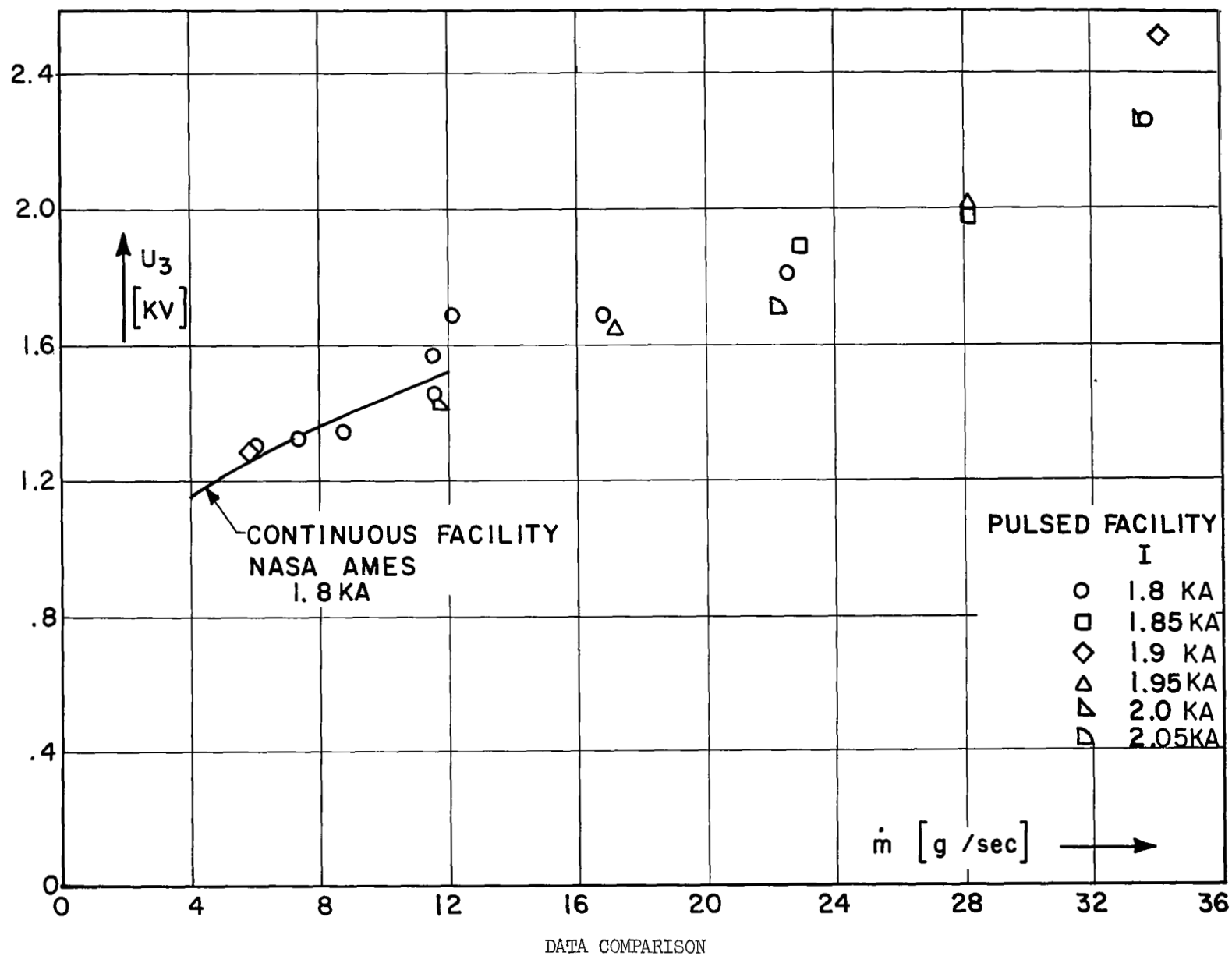


Fig. 20. Voltage between cathode and 54" station  $U_3$  as function of nitrogen flow rate  $\dot{m}$ .

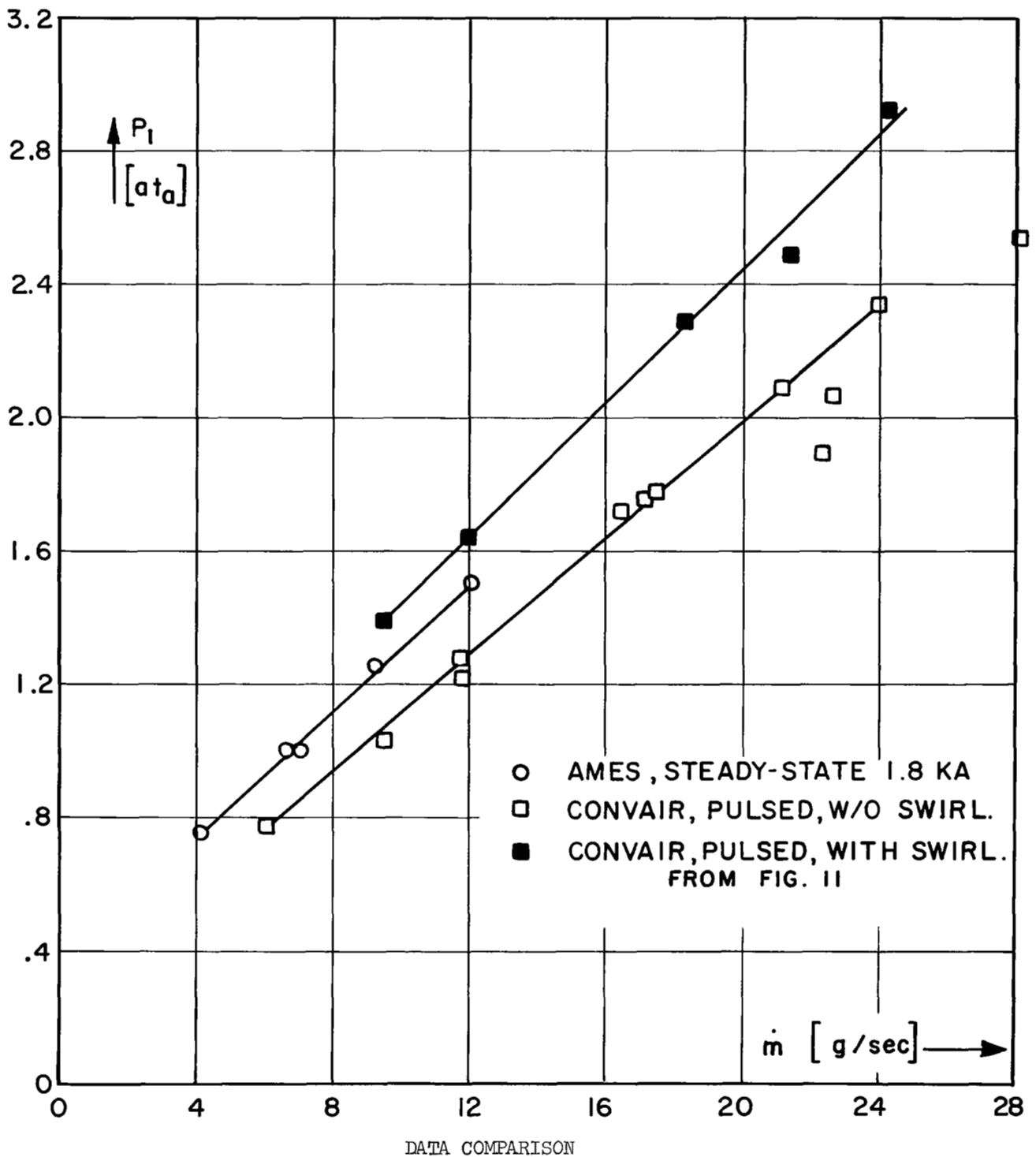
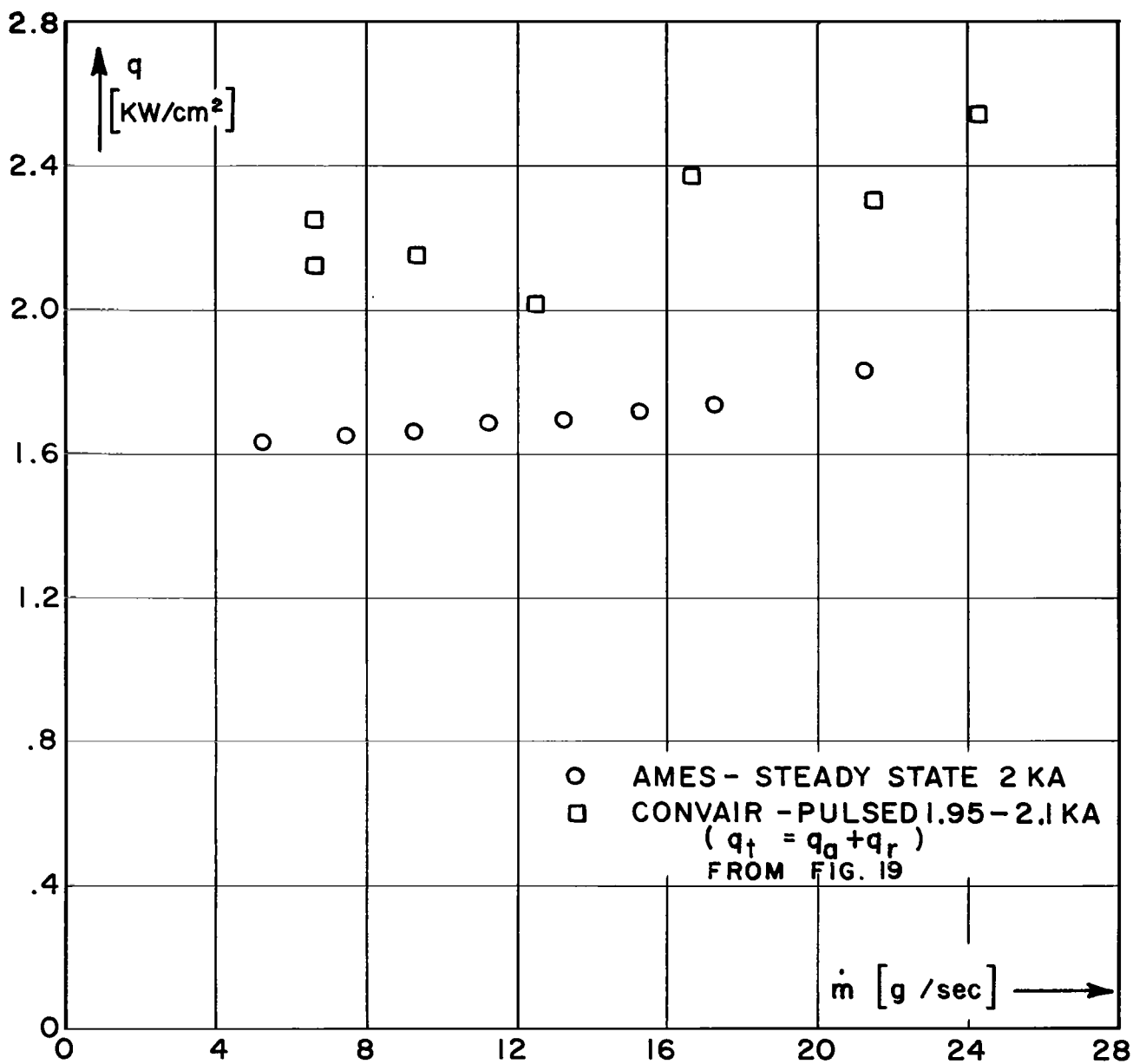


Fig. 21 Inlet pressure  $P_1$  as function of nitrogen flow rate  $\dot{m}$ .





DATA COMPARISON

Fig. 22. Total heat flux to constrictor wall  $q_t$  as function of nitrogen flow rate  $\dot{m}$ .

#### 4. Photographic Investigations

The pulsed arc facility is particularly suitable for photographic observations because the quartz walls allow a direct optical access. All high speed photos were taken with 1  $\mu$ sec exposure time.

(A) Cathode phenomena.- The cathode is placed at the inlet to the arc constrictor. Any erosion therefore produces a contamination of the gas stream. In order to minimize cathode erosion, three different cathode versions were tested. These are shown in Fig. 23.

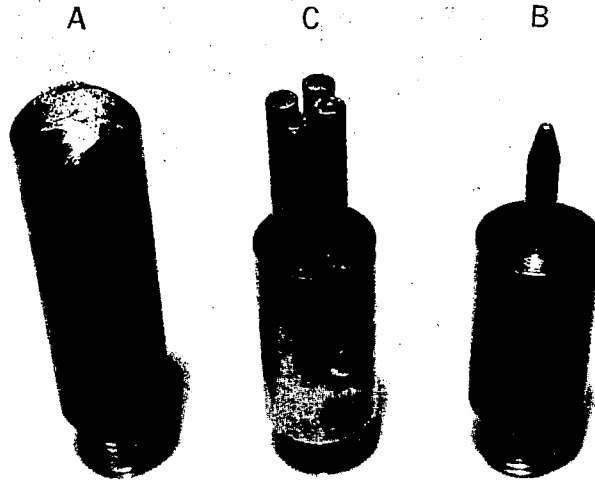
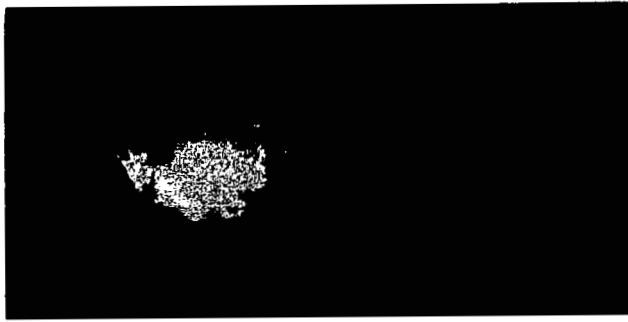


Fig. 23. Different cathodes tested with the pulsed arc.

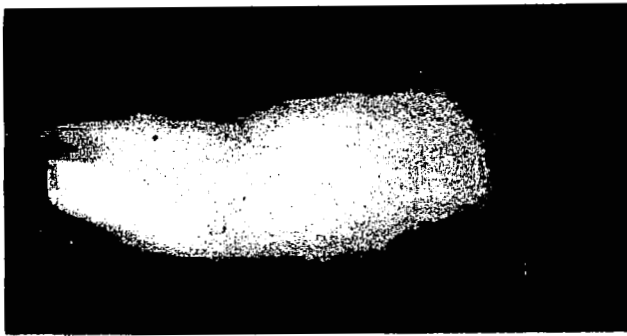
Cathode A is a 1/2"-diameter copper rod with a spherical end face. As one might have expected, because copper is not able to sustain appreciable thermionic electron emission, this cathode showed heavy erosion after a single exposure to the pulsed arc. (For a tabulation of the relative resistance of various metals to erosion by arc attachment see Ref. 11).

Figure 24 shows that the arc attachment on the cold copper cathode is constricted. The photos of Fig. 24 were taken about 3 msec after the start of the arc.

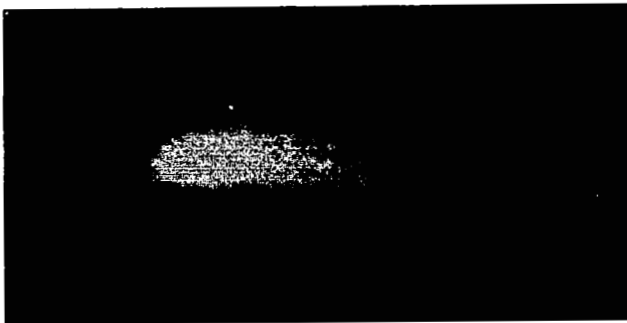
Cathode B consists of a single rod of 1/8"-diam. thoriated tungsten. The cathode photographed in Fig. 24 had a flat face and was not tapered as is shown in Fig. 23. The photo 24B shows a Maecker cathode jet which is bent sideways. In other high speed films it was observed that this cathode jet can either be bent or straight. Note that the current return along the arc constrictor is not truly coaxial. Two wires at about equal distance on opposite sides of the arc constrictor carry the return current. The asymmetry of the magnetic field produced by the current return path probably causes the current carrying cathode jet to bend.



A  
1/2" SPHERICAL  
COPPER CATHODE



B  
SINGLE PIN  
1/8" TUNGSTEN  
2% THORIATED



C  
4 PIN CATHODE OF  
1/8" TUNGSTEN  
2% THORIATED

—→ | 1 cm | ←—

Fig. 24. Arc attachment on the three cathodes of Fig. 23.  
17.5 g/sec nitrogen flow, 3.2 KA.

The cathode C consists of four tungsten rods pressed into a copper slug. This type of cathode showed the smallest amount of erosion of the three versions. In Fig. 24C no cathode jets or constricted attachment are visible in the side-on view. In order to detect further details of the arc attachment on the four-pin cathode, a film was taken with a  $45^\circ$  end-on view. A selected sequence of 3 frames from this film is shown in Fig. 25.

When steady flow conditions have been reached at  $t = 4.5$  msec, we see that the cathode attachment occurs simultaneously on the various tungsten rods. Preferentially the sharp edges of the flat end faces are highly luminous, indicating the position of the arc attachment. No evidence for a cathode jet can be seen. These photos indicate that a cathode design with many parallel tungsten rods may be feasible, where each rod carries its share of the total arc current. The arc attachment on a single  $1/8$ " tungsten rod with 2% thorium and a pointed end face is shown in Fig. 26. A straight cathode jet is clearly visible in every frame of that film. On similar films it was observed that the length of the luminous jet increases with increasing current and decreasing pressure.

(B) Diameter and instabilities of the arc column.- In the following discussion the pattern of high luminosity in the constrictor is taken as an indication of the arc diameter. It is safe to assume that a localized region of high luminosity in a dense gas also corresponds to the position of the electric current. Yet, a uniform region of high luminosity does not necessarily imply uniform temperature or current density, because (a) these parameters are not simply related and (b) a uniform luminosity can appear on the film due to overexposure.

Figure 27 shows a time sequence of photos which display the different phases of the pulsed arc interacting with an axial gas flow in a constrictor.

$$t = 0$$

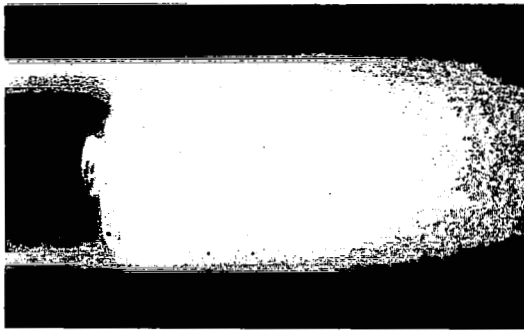
The wire has exploded in the center of the tube. The metal plasma is expanding radially outwards.

$$t = 0.2, 0.84, 1.75 \text{ msec}$$

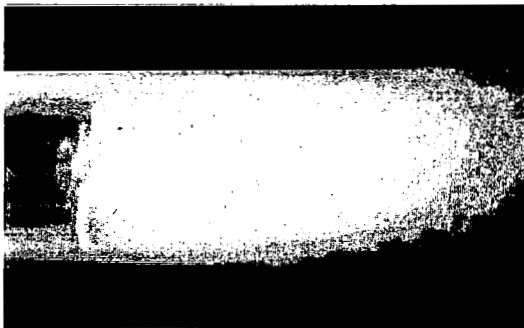
Pressure is building up due to ohmic heating of the metal and nitrogen plasma. The gas is accelerated in the axial direction.

$$t = 2.64, 3.9, 4.9 \text{ msec}$$

The quasi-steady flow of nitrogen gas through the constrictor has been established. The metal plasma is swept out of the tube. The axial flow



$t = 1.17 \text{ msec}$



$t = 4.5 \text{ msec}$



$t = 5 \text{ msec}$

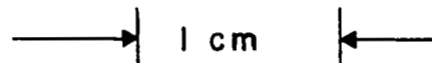


Fig. 25. Arc attachment on the cathode of Fig. 23C, 17.4 g/sec nitrogen flow, 3.0 KA,  $t = 0$  at start of the current pulse.

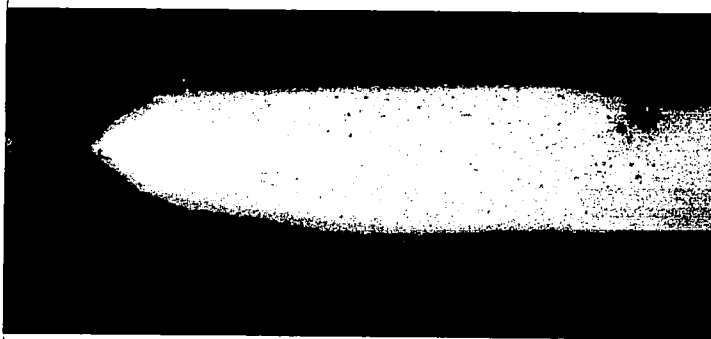
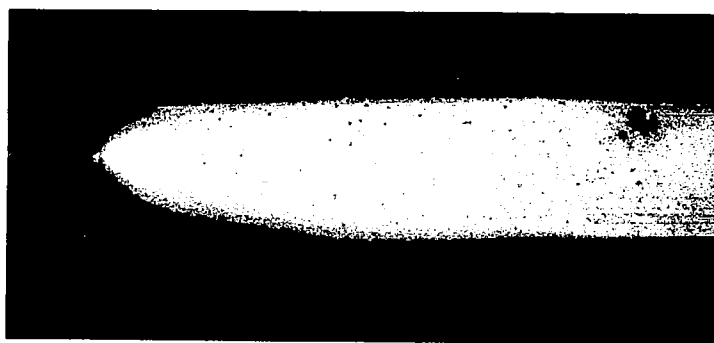


Fig. 26. Arc attachment on the cathode of Fig. 23B with pointed end face. 16 g/sec nitrogen flow, 2 KA, lower photo is retouched in order to show the cathode jet more clearly.

of nitrogen constricts the arc to a diameter which fills about 1/2 of the tube. The arc diameter is not constant. Kink and twisting instabilities appear to be present.

$$t = 5.7 \text{ msec}$$

The arc current is down to a low value. This is near the end of the pulse. The arc has decreased its diameter. It is interesting to note that parallel arc filaments seem to exist. The displayed frames are typical ones selected out of a high speed film of about 80 frames.

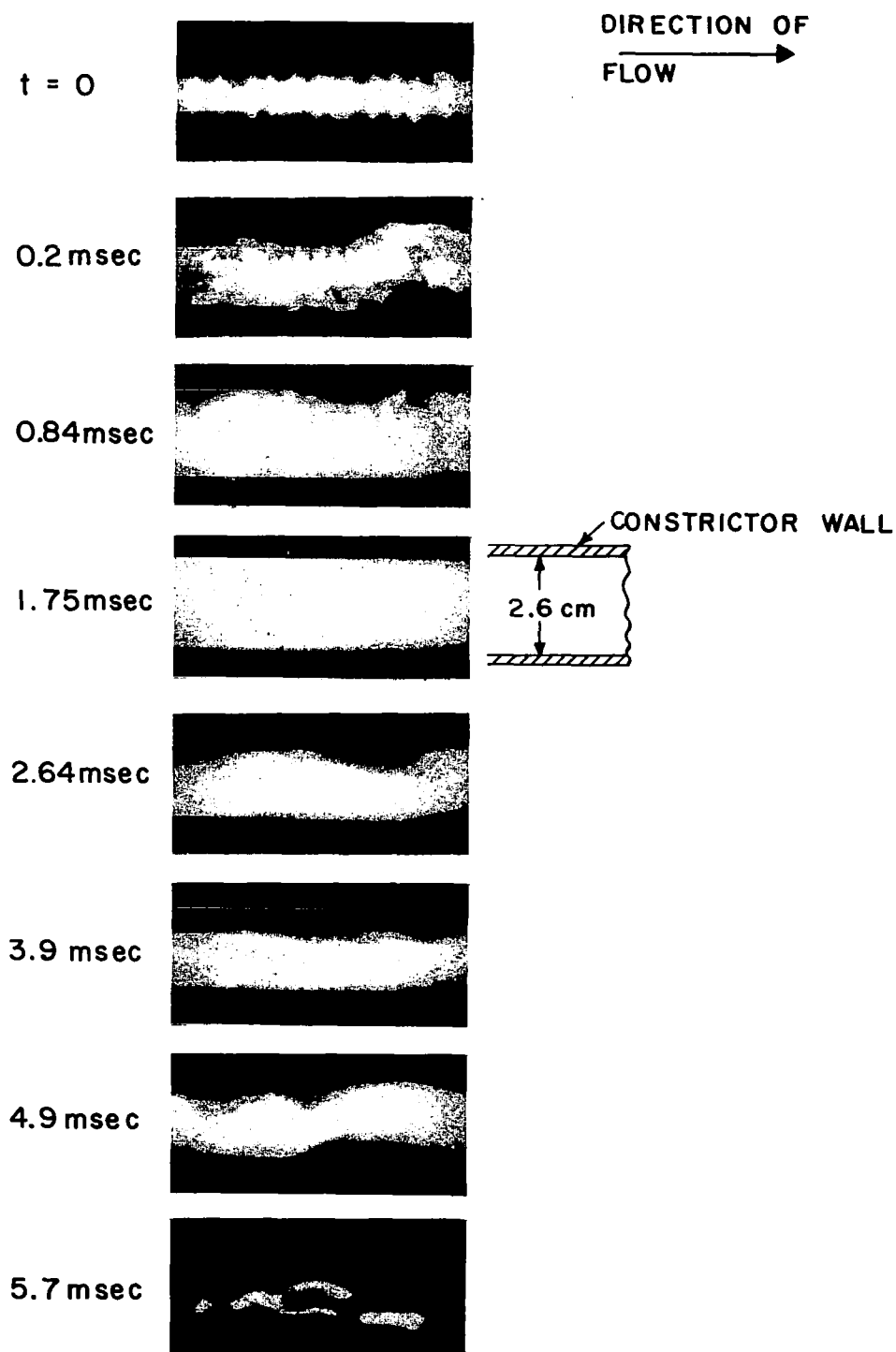


Fig. 27. High speed film displaying the time history of the pulsed arc with axial flow. 11 g/sec nitrogen flow, 2 KA. Position about 20 cm downstream of cathode.

Figure 28 shows a larger portion of the inlet section to the arc constrictor. Figure 28 also was taken at a higher flow rate of nitrogen. At a higher flow rate the arc constricts to a smaller diameter, which makes the instabilities more pronounced.

$$t = 0$$

The trigger wire explodes.

$$t = 0.73, 1.26 \text{ msec}$$

This is the high pressure transient phase of the flow. The cold nitrogen flow enters the constrictor from the left. The contact of this cold flow with the arc causes the arc to constrict. One can observe that the constriction progresses from the left to the right.

$$t = 2.9, 3.5 \text{ msec}$$

This is the steady phase of the arc flow interaction. The arc at high flow rate is constricted to about  $1/4$  of the tube diameter. The arc shape is very crooked.

$$t = 5.7 \text{ msec}$$

This is near the end of the pulse. With decreasing current, the arc diameter decreases.

Figure 29 demonstrates how well the arc instabilities can be eliminated by swirling the gas flow through the constrictor. A strong vortex is generated in the flow by blowing the gas in tangentially. At high flow rate with a strong vortex the arc is constricted to a narrow straight line.

High speed films taken of the arc near the anode show a nearly uniform luminosity across the whole diameter of the tube, even at 46 g/sec nitrogen flow with 1.9 KA current. Films taken in the middle section of the constrictor indicated that the arc column did not fill the constrictor completely.

(C) Luminosity pattern or bodies in the exhaust stream.- A few films were taken of the luminous patterns created when the exhaust stream interacts with a solid body. The unperturbed exhaust stream shows a relatively low luminosity. The background pressure in the exhaust region was in the order of 100 mm Hg. Before every discharge, the glass tube, comprising the exhaust volume, was pumped down to a pressure of about 1 mm Hg. The interaction of the exhaust flow with a wedge is shown in Fig. 30.

The luminous region corresponds to the high density flow behind the shock wave. The luminous region does not extend to the sharp edge of the wedge. The forward boundary of the luminous region does not necessarily correspond the position of the shock wave. Therefore, it is not safe to conclude the Mach number of the flow from the magnitude of the observed angle



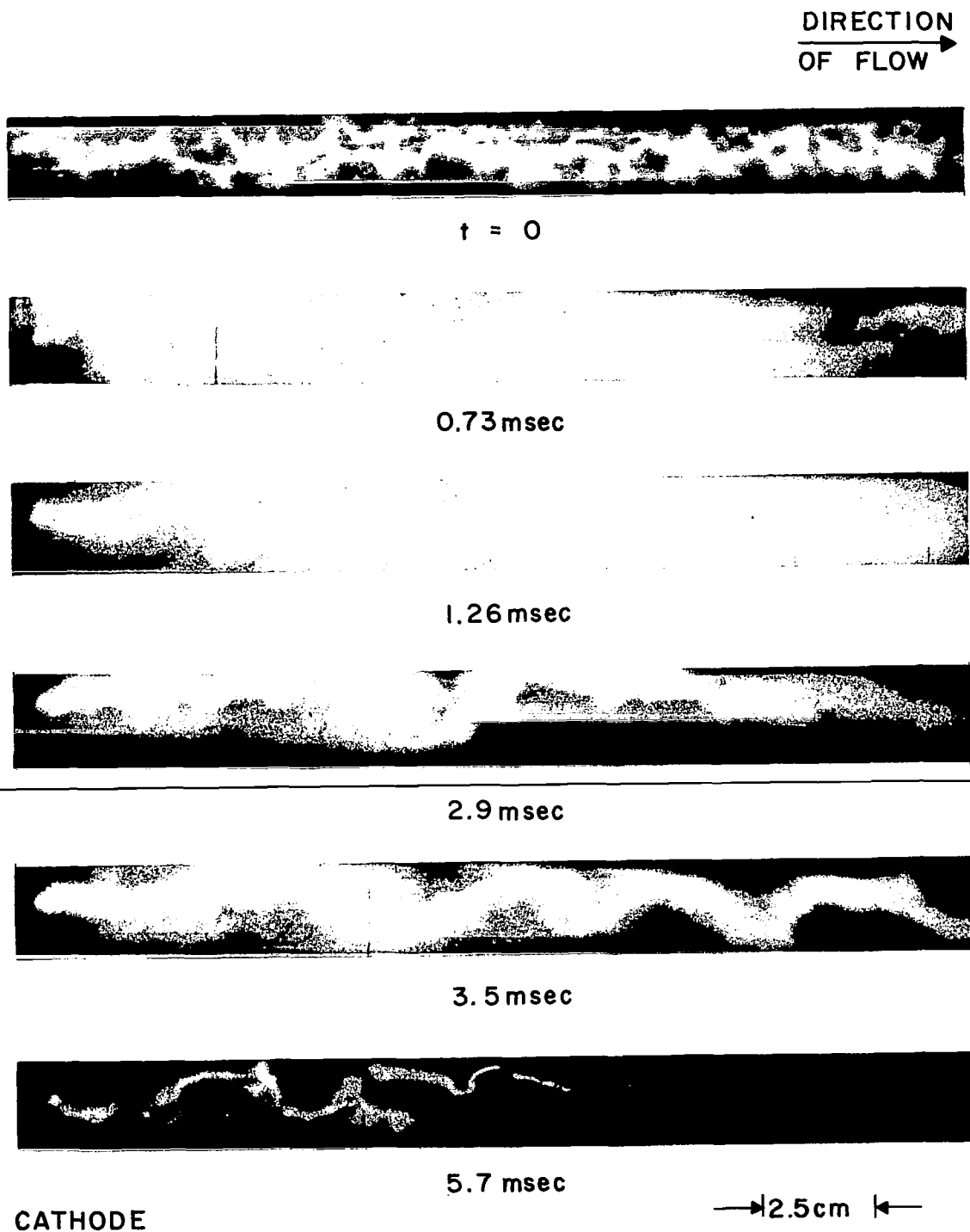
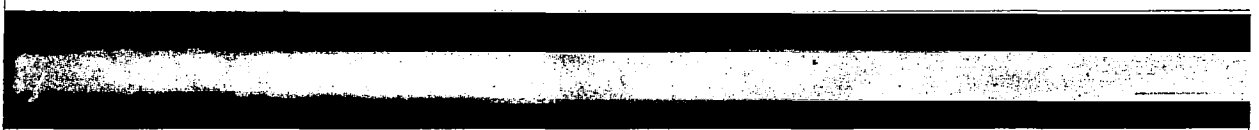


Fig. 28. High speed film displaying the time history of the pulsed arc with axial flow. 39 g/sec nitrogen flow, 1.9 KA. Position at the cathode end of the constrictor.

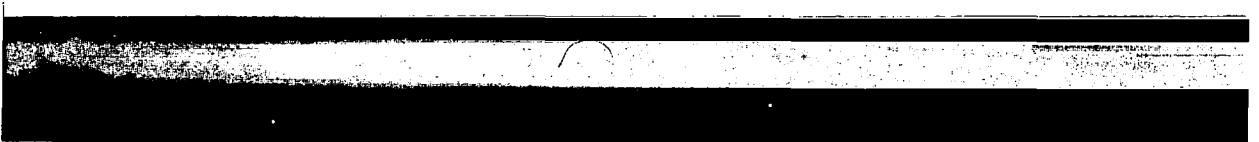
DIRECTION  
OF FLOW →



$t = 0$



1.06 msec



4.0 msec



4.65 msec

→ 1.8cm ←

CATHODE

Fig. 29. High speed film displaying the time history of the pulsed arc with axial flow containing a strong vortex. 46 g/sec nitrogen flow, 1.9 KA. Position at the cathode end of the constrictor.

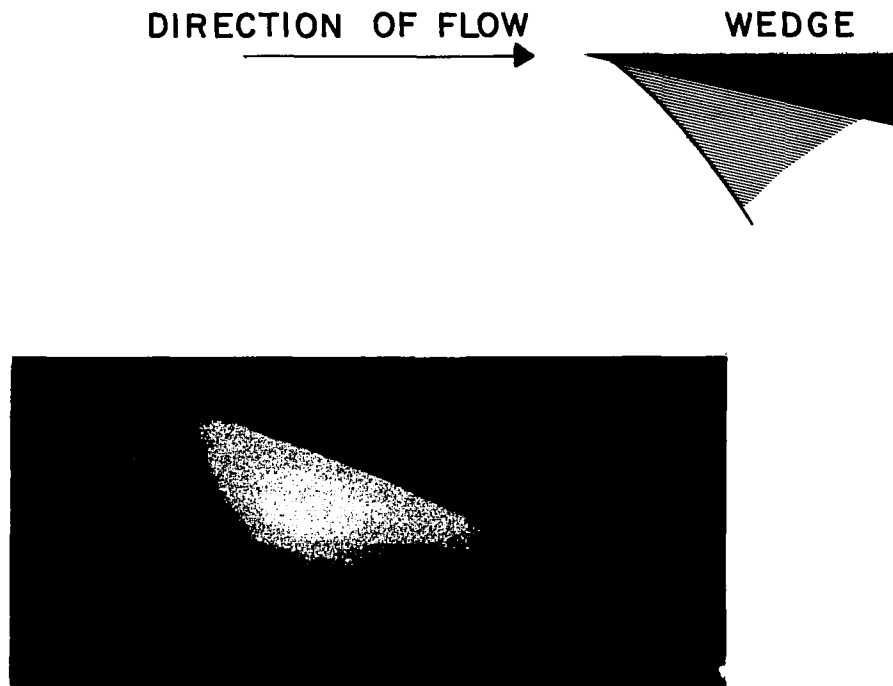


Fig. 30. A wedge exposed to the exhaust stream of the pulsed arc heater. Position of leading edge about 4 cm from exit plane of anode. 30.7 g/sec nitrogen flow, 3.5 KA current, exposure time about 1  $\mu$ sec.

between the direction of the flow and the luminosity pattern. From the nearly straight boundary line between the luminous region and the oncoming flow one can conclude that the exhaust flow is supersonic. From the expansion ratio of the anode nozzle one would expect a Mach number of about three.

In order to check on the steadiness of the exhaust flow a high speed film was taken of the exhaust interaction with a blunt body. A few of the frames are shown in Fig. 31. One expects a curved shock to exist in front of a blunt body in a supersonic flow. The photos show the luminous region behind that shock. On the film strip one can observe that during the last 3 msec of the pulse-heated flow, a very steady luminous region exists in front of the blunt body. This lends evidence to the belief that during the final phase of the current pulse a quasi-stationary flow is obtained.

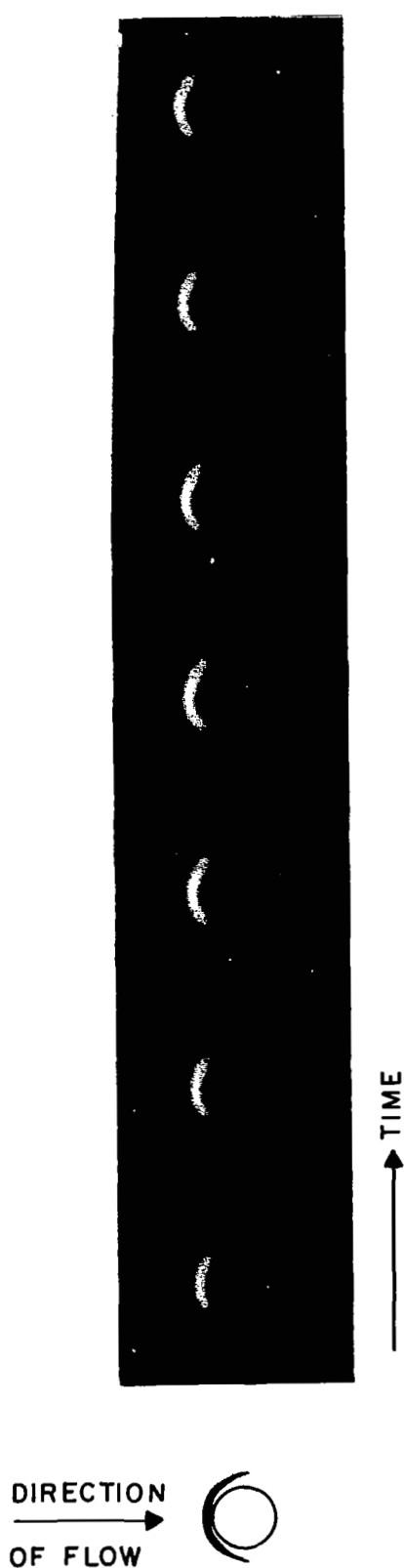


Fig. 31. A 0.5"-diam. rod exposed crosswise to the exhaust stream of the pulsed arc constrictor. Position about 2 cm from exit plane of the anode. Frame separation about 80  $\mu$ sec, exposure time about 1  $\mu$ sec.

#### IV. CONCLUDING SECTION

The main purpose of this study was to investigate the feasibility of obtaining stationary flow conditions with a constrictor length and pulse time of the given magnitude.

The processes leading to a quasi-steady flow in the pulsed arc constrictor can be understood with a knowledge of non-steady flow in compressible fluids. The following is a short description of the effects taking place, and an initial estimate of the time needed to reach quasi-steady flow.

First, consider the phenomena occurring at the time of arc initiation. The thin trigger wire in the center of the constrictor explodes within a few microseconds after the ignitrons are fired. A strong shock wave propagates with supersonic velocity radially outward until it hits the constrictor walls after a time of less than  $40 \mu\text{sec}$ . The shock wave is reflected at the constrictor walls and travels radially inward. These radial shock waves decay in less than  $200 \mu\text{sec}$ , and therefore should not delay establishment of steady flow.

Some data exist in the literature on the time constants of arc-adjustment to a sudden change in arc current. Reference 6 reports experimentally determined time constants of a 1-amp. nitrogen arc ranging from  $120 \mu\text{sec}$  at  $1/2$  atm pressure to  $420 \mu\text{sec}$  at 3 atm. Other gases, including air, show a faster response than nitrogen. A theoretical analysis in Reference 7 considers specifically the case of a constricted arc with axial flow. For a constrictor tube with a radius of 1 cm a relaxation time of about  $500 \mu\text{sec}$  is indicated. These experiments were performed with a small current modulation on a low current arc. In the analysis of Reference 7 radiation was neglected. One, therefore, can assume that the actual response time of a high current arc will be faster than indicated by the references. The transient time of the pulsed, constricted arc heater should therefore be governed by gasdynamic effects.

The establishment of the arc creates a high pressure plasma which is traversed by waves propagating in the axial direction. These are essential for establishing the quasi-steady state. The speed of these axial waves is governed by the speed of sound in the gas. A high sound speed is obtained by a high temperature and a low molecular weight. The exploding wire, therefore, is made from a light metal like aluminum. In comparable wire explosions initial temperatures in the range of  $5 \cdot 10^5$  °K have been measured.<sup>8</sup> The mass of a 5 mil aluminum wire  $5\frac{1}{4}$ " long is about  $5 \cdot 10^{-2}$  g, while the total amount of air contained in the 1"-diam. constrictor is about 0.7 grams at atmospheric conditions. The energy needed to explode the wire is about 1K Joule. If initially 30 KJ are available to heat an arc column containing 0.3 g of nitrogen the enthalpy will be  $10^5$  Joules per gram. According to Reference 9 this corresponds to a temperature of 14,000 °K. At this temperature under atmospheric pressure the plasma is fully dissociated.

Choosing an average molecular weight of  $M = 18$  we can estimate the speed of sound  $c = \sqrt{\gamma RT} = 3.300 \text{ km/sec.}$

where  $\gamma = 5/3$ , ratio of specific heats for a monatomic gas

$$R = \text{Gas constant } 8.3149 \cdot 10^3 \frac{\text{Joules}}{\text{kg mole } ^\circ\text{K}} .$$

After the arc is established, the constrictor is filled with a high pressure, high temperature gas. The gas flow has not yet had time to adjust. Initially rarefaction waves start travelling with the speed of sound from the open end into the constrictor thus accelerating the gas. At the open end the gas is exhausted with sonic velocity. Gas is fed at constant mass flow rate to the constrictor through the sonic orifices. Waves reaching the back wall of the constrictor are reflected. When they again reach the sonic outflow region of the constrictor channel, they are carried outside. The details of the wave interactions can be calculated with the method of characteristics.

In the present case the situation is complicated by temperature gradients. Also a one-dimensional treatment may not be adequate. Therefore, only an estimate of the relaxation time will be obtained by comparing the present case with similar problems of unstationary gas dynamics.

In Reference 4, Vol. II, p. 983 it is calculated that a flow starting in a tube with similar boundary conditions needs a relaxation time equivalent to about 4.5 transit times of a sonic wave until essentially steady flow is obtained at both ends. With a sonic speed of  $c = 3.300 \text{ km/sec}$  and a constrictor length of 137 cm this leads to a transient time of  $t = 1.9 \text{ msec}$  in our case. This estimate is in reasonable agreement with the experiments.

The best indication of a steady flow is a constant inlet pressure level. This has been obtained for times up to 3 msec. The transient phase of the flow lasted for about 2.5 msec. The constant pressure level was particularly well defined for the lower range of mass flow rates and also if gas breakdown triggering is used. If gas breakdown triggering is used, the gas experiences an axial acceleration prior to the main current pulse. The low current arcs which are drawn to the various copper segments are effective in reducing the transient time and the initial pressure overshoot. A strong vortex in the gas flow appears to increase the transient time. This may be due to an interaction of the expansion waves with the vortex. The comparison between data taken on the pulsed facility and those taken under similar condition on the continuous arc heater at the NASA Ames Research Laboratory has indicated that the measured arc voltages agree closely in magnitude and trend of the data. No pronounced effect of the gas swirl on the measured arc voltage was found. The inlet pressure measured on the pulsed facility without a gas swirl was generally lower than the steady-state data. Note that the NASA Ames facility introduces the gas into the constrictor with a moderate amount of swirl. However, the range of pressures on the pulsed facility with and without swirl (Fig. 11) spans the steady-state data when corrected for a small difference in

constrictor diameter (Fig. 21). The deviation of the pressure data therefore can be attributed to differences in the gas injection used in the two facilities.

The relatively large scatter of the pulsed data is in part due to the uncertainty involved in evaluating oscilloscope traces. But beyond that, there may be reasons inherent in the operation of the device. In particular the inlet pressure is very sensitive to the exit area in that position where choking occurs. Due to Joule heating of the flow, the position of choking could have extended into the diverging section of the anode. Inspection of the anode reveals that the current attachment occurred at the straight exit wall and at the diverging nozzle wall. The attachment tracks form streamers which extend from the straight section into about one-half of the diverging section. This indicates one or more attachment spots which probably moved downstream within the anode. Some inlet pressure traces at high flow rate showed fluctuations which could have been caused by changes in the position of choking.

The high speed films have given evidence for the existence of the Maecker cathode jets. Under the present conditions these cathode jets seem to be an important factor in the behavior of the constrictor inlet section. These jets appear to increase in length with increasing current and decreasing pressure. They are not always coaxial with the arc. These jets can shoot forward at a slanted angle relative to the axis of the arc, particularly if the cathode surface is irregular or if the magnetic field is asymmetric in the cathode region.

These jets contain extremely hot gas, because they originate at a point of very high current density. When these jets impinge on the quartz wall, localized erosion is generated. This form of erosion has been observed on the quartz wall in the form of spear-like tracks which extend from the position of the cathode. In a continuously operating arc heater with a constrictor wall made from copper segments, these jets could short out these segments electrically. Shorting of the segments and destruction near the cathode actually is reported in the literature.<sup>2,10</sup>

The cathode jets could also play a role in exciting the observed arc instabilities. The stabilizing effect of a swirling gas injection is well known. In the present study a direct photographic evidence for this effectiveness was obtained. It appears that some further experimentation with a vortex of variable strength would be of value.

When the four-pin thoriated tungsten cathode was tested it was hoped that this would reduce the cathode erosion rate. But one could not a priori assume that the arc would attach on more than one pin simultaneously. The photos of Fig. 22 demonstrate that parallel and simultaneous cathode attachment actually occurs without the use of ballast resistors. The attachment occurs on the sharp corners at the flat face of the 1/8"-diam. tungsten pins. This rather diffuse attachment eliminates the cathode jets. It is likely that the close spacing of the tungsten pins is an important factor in obtaining parallel attachment.

## V. REFERENCES

1. V. R. Watson and E. B. Pegot, "Numerical Calculations for the Characteristics of a Gas Flowing Axially through a Constricted Arc," NASA Technical Note TND-4042 (1967).
2. C. E. Shepard, D. M. Ketner, J. W. Vorreiter, "A High Enthalpy Plasma Generator for Entry Heating Simulation," Paper presented at the Institute of Environmental Sciences, Washington, D. C. 1967.
3. G. N. Glasoe and J. V. Lebacqz, Pulse Generators, Dover Publ. (1965).
4. A. H. Shapiro, The Dynamics and Thermodynamics of Compressible Fluid Flow, Ronald Press Co., N. Y. (1953).
5. C. D. Hodgman, Ed., Handbook of Chemistry and Physics, 37th Ed., Chemical Rubber Publishing Co., Cleveland, Ohio.
6. K. H. Yoon and H. E. Spindle, "A Study of the Dynamic Response of Arcs in Various Gases," Trans. AIEE, Power Apparatus and Systems, Vol. 77, p. 1634 (1954).
7. D. A. Prelewicz and D. M. Benenson, "Nonsteady Coaxial Arcs in Fully Developed Plasma Flow," AIAA Journal Vol. 5, No. 7, p. 1320 (1967).
8. W. G. Chace and H. K. Moore, Exploding Wires, Vol. III, Plenum Press, N. Y. (1964).
9. F. Burhorn and R. Wienecke, "Plasmazusammensetzung, Plasma Dichte, Enthalpie und spez. Wärme von Stickstoff, Stickstoffmonoxyd und Luft." Zeitschr. f. Phys. Chemie 215, p. 269-286 (1960).
10. G. L. Cann, R. L. Harder, and G. L. Marlotte, "Interaction Phenomena between Coaxial Arcs and High Speed Gas Flows," AIAA Fluid and Plasma Dynamics Conference, Los Angeles, June 1968, Paper 68-707.
11. R. Dethlefsen, "Investigation of Electrode Erosion in High Current Electric Arcs," Interim Contract Report prepared for Thermomechanics Research Laboratory, ARL, OAR, Wright Patterson Air Force Base, Ohio. To be printed as ARL-Report 1968.